

POLITECNICO DI TORINO

**Corso di Laurea Magistrale
in Ingegneria Energetica e Nucleare**

Tesi di Laurea Magistrale

**Methanol synthesis through CO₂
hydrogenation: reactor and process
modelling**



Relatori

prof. Massimo Santarelli

dott. Emanuele Giglio

dott. Domenico Ferrero

Candidato

Francesco Calogero

Dicembre 2018

Index

| | |
|--|-----------|
| 1. INTRODUCTION | 1 |
| 1.1. APPLICATION CONTEXT | 1 |
| 1.2. METHANOL ECONOMY AS A POSSIBLE SOLUTION | 5 |
| 2. CO₂ HYDROGENATION: FROM RESOURCES TO METHANOL | 9 |
| 2.1. H ₂ PRODUCTION | 9 |
| 2.2. CO ₂ CAPTURE | 11 |
| 2.3. CO ₂ HYDROGENATION | 13 |
| 2.3.1. <i>Overview</i> | 13 |
| 2.3.2. <i>Process tuning</i> | 14 |
| 2.3.2.1. Catalyst | 14 |
| 2.3.2.2. Thermodynamic parameters – kinetic parameters – catalyst combined effect | 15 |
| 2.3.2.3. Products' separation and recycle | 16 |
| 3. MODELLING OF A METHANOL PRODUCTION PLANT IMPLEMENTING CO₂ HYDROGENATION AND H₂O ELECTROLYSIS | 17 |
| 3.1. THERMODYNAMIC EVALUATION OF CO ₂ HYDROGENATION | 17 |
| 3.2. STUDY OF CO ₂ HYDROGENATION AT REACTOR LEVEL | 23 |
| 3.2.1. <i>Simulation of the reactions participating to CO₂ hydrogenation</i> | 24 |
| 3.2.1.1. Model definition | 24 |
| 3.2.1.2. Catalyst morphology | 26 |
| 3.2.1.3. Fluid physical properties | 26 |
| 3.2.1.4. Global mass transfer coefficient | 29 |
| 3.2.1.5. Experimental set up | 30 |
| 3.2.1.6. Implemented kinetics | 32 |
| 3.2.1.7. Simulation and results | 33 |
| 3.2.2. <i>Definition of a power-law kinetic scheme</i> | 38 |
| 3.3. PLANT'S SIMULATION AND EVALUATION | 41 |
| 3.3.1. <i>Design of the plant</i> | 41 |
| 3.3.1.1. Initial decisions | 41 |
| 3.3.1.2. Simulation on Aspen Plus [®] | 43 |
| 3.3.2. <i>Plant efficiency assessment</i> | 45 |
| 3.3.2.1. Chemical power of produced methanol | 46 |
| 3.3.2.2. Electrical power used to produce methanol | 46 |
| 3.3.2.3. Efficiency calculation and considerations | 50 |
| 4. CONCLUSIONS | 51 |
| APPENDIX: ELECTROLYSER'S THERMAL BALANCE | 52 |
| REFERENCES | 54 |

Abstract

Since the fossil sources are finishing and the effect of the CO₂ accumulation in the atmosphere is becoming even more evident, the CO₂ re-use is a topic of primary importance. In this field, a solution could be the CO₂ hydrogenation. This thesis has the purpose of the determination of a reactor kinetics scheme and its use for the modelling of a plant realizing the CO₂ hydrogenation by means of H₂ obtained by water electrolysis and captured carbon dioxide.

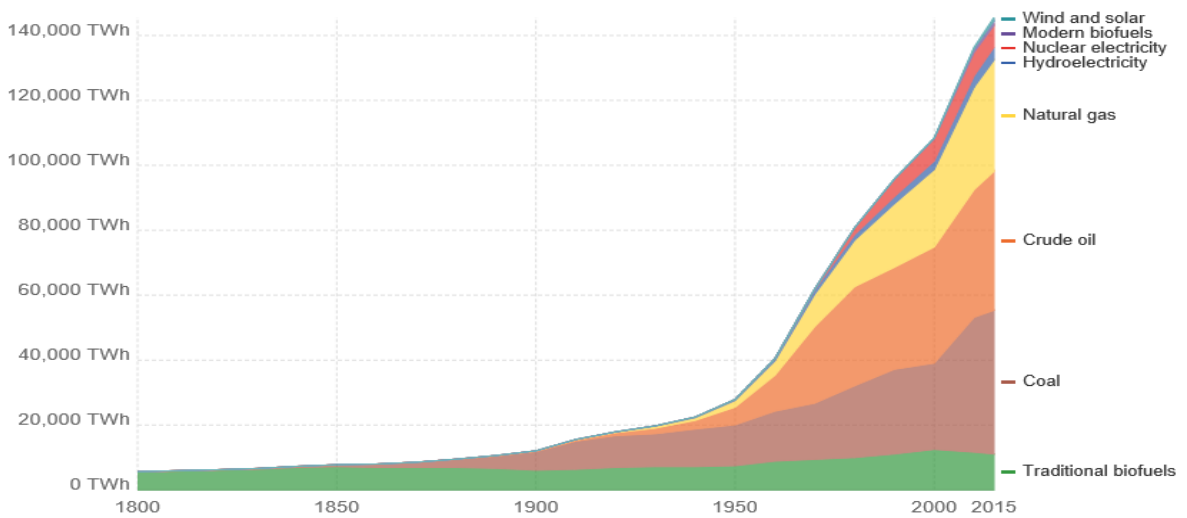
1. Introduction

1.1. Application context

The actual socio-economical system is strongly linked to the use of fossil sources, employed as fuel (for energetic purposes) or raw materials. Regarding the topic of Energy, the connection can be traced back to the invention of the steam engine, fed by coal; this was one of the events promoting the Industrial Revolution, which started in the second half of the XIX century (contributors, 2018). The Revolution led to a society characterized by an ever-increasing need for energy, so that wood (previously, predominant) was no longer enough. Firstly, it relied on coal to meet the new energy demand; with the advent of the Second Industrial Revolution, oil entered the energy landscape; by the end of the century, two other important sources, natural gas and hydropower, appeared. The two World Wars (particularly, the Second one) generated an increase in the consumptions' growth rate, which was supported mainly by the fossil fuels; in that historical period, oil and natural gas began the rise that would bring them, in the future, to be comparable to coal. The growth phase triggered by the Second World War continued until today, with the other energy sources (hydropower, nuclear, solar, wind, and modern biofuels) having a marginal role (contributors, 2018; Ritchie & Roser, 2017). In 2016, primary energy consumption was largely met by fossil fuels (almost 85.5%): mainly oil (33.3%), followed by coal (28.1%) and natural gas (24.1%) (British Petroleum Company, 2017).

Global primary energy consumption, 1800-2015

Global primary energy consumption by source, measured in terrawatt-hours (TWh).

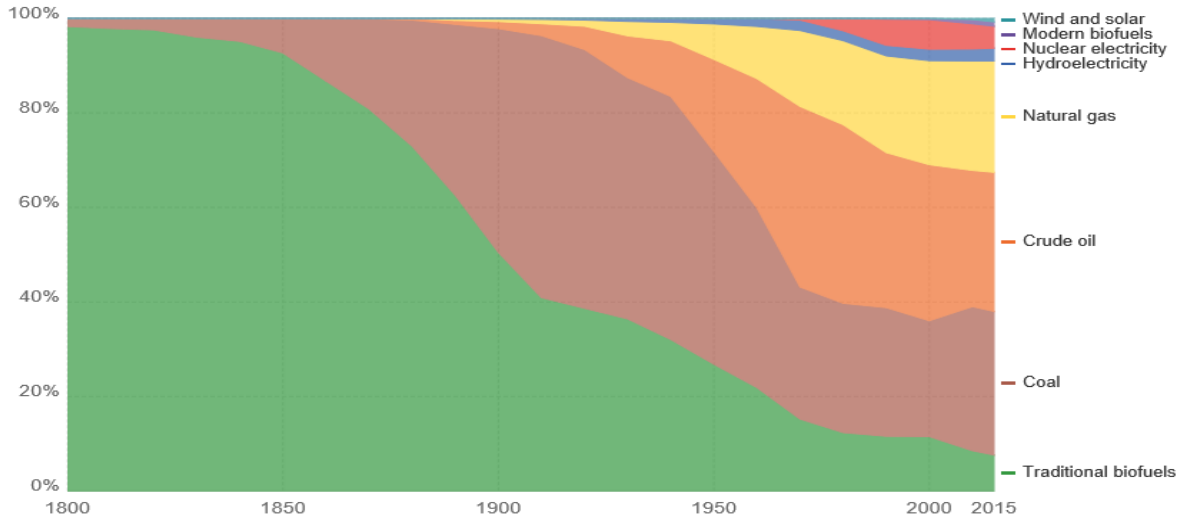


Source: Vaclav Smil (2017), Energy Transitions: Global and National Perspectives

Figure 1.1: Global Primary Energy Consumption, 1800-2015. Taken from (Ritchie & Roser, 2017).

Global primary energy consumption, 1800-2015

Global primary energy consumption by source, measured in terrawatt-hours (TWh).



Source: Vaclav Smil (2017), Energy Transitions: Global and National Perspectives

Figure 1.2: Percentage of Global Primary Energy Consumption satisfied by each source. Taken from (Ritchie & Roser, 2017).

However, a system based mainly on a single base is largely affected by its negative aspects. Thus, some weak points¹ of the actual socio-economical system are (contributors, 2018):

¹ The considered aspects are those on which the subject of this thesis has an effect. It is suggested to visit (contributors, 2018) for a much exhaustive list.

- *Non-renewable nature of the fossil sources*: for real, they regenerate over periods of time much longer than the duration of human life; for this reason, they are considered non-renewable. A rough estimate² of the duration of each one of them can be obtained, for a single year, by the ratio Reserves/Production (R/P, [year]) between the established reserves (R, [TWh]) at the end of the annuity and the annual mean production (P, [TWh/year]). Such a kind of analysis has led to the conclusion that remaining coal, oil and natural gas could last 153, 50.6 and 52.5 years respectively (British Petroleum Company, 2017; Ritchie, 2017);
- *CO₂ emissions derived from the combustion of fossil fuels*: The *Greenhouse effect* is the atmospheric temperature rise due to the accumulation in the atmosphere of gasses which are transparent to solar radiation (that reaches the surface and heats it up), but opaque to infrared one emitted by the Earth's crust as a result of the heating. These gasses are referred to as *Greenhouse Gasses (GHG)*. The most used method for the conversion of the chemical energy contained in fossil resources is combustion; this reaction produces several GHG, particularly carbon dioxide. According to British Petroleum's estimates (British Petroleum Company, 2017), in 2016, 33432 million tons of CO₂ were emitted (for energy purposes), corresponding to an increase of 0.1% with respect to the previous year; moreover, during the decade 2005-2015, there was a mean annual growth rate of CO₂ emissions of 1.6%. An emission of this entity is not compatible with the targets of containment of the temperature rise foreseen by recent international agreements: the Paris Agreement (which came into force on 4 November 2016) requires the involved nations to implement policies of reduction of the emissions of Greenhouse gasses "*to limit global warming to well below 2°C above pre-industrial levels – and pursue efforts to limit the temperature increase to 1.5°C*" (European Commission, Secretariat-General, 2016). However, in (Mcsweeney & Pearce, 2016), it is shown that, at the publication of the article (May 2016), basing on the emissions of the previous years, only 5.2 and 20.3 years respectively remained to reach the threshold of 1.5 °C and 2 °C (with a probability of 66%).

In conclusion, the most limiting aspect is the emission of carbon dioxide.

To prevent the looming crisis, it is needed a *decarbonization* of the global economy, accompanied by a more efficient use of the produced energy. Its main points are (Ritchie & Roser, 2017):

- *Reduction of the CO₂ production by the substitution of fossil fuels with renewable sources and nuclear power*: these alternatives are not characterized by null CO₂ emissions: during the construction of the plants and the functioning of the auxiliary systems, a certain amount of carbon dioxide is released. However, this quantity is much lower than that emitted using fossil fuels;
- *CO₂ capture as a part of CCS or CCU techniques*: the possibility to act on emissions, either directly downstream the source (anthropic or natural) and at the impact target (atmosphere), is very interesting. Among these two levels of intervention, there is a very important difference, which consists in the concentration of the carbon dioxide that has to be processed: the

² Since both Reserves and Production are characterized by time variations, due to aspects like the technological evolution and the consumptions

atmospheric agents tend to dilute the CO₂ (Olah, et al., 2009). The capture at the atmospheric level is not yet viable, since adequate technologies are not available. In this field of application, one of the most interesting solutions is the use of basic absorbent (NaOH, KOH, Ca(OH)₂), which absorb carbon dioxide in an exothermic way. However, their regeneration is an endothermic process with an excessive need (Olah, et al., 2009). The capture at the source is at a more advanced stage. It is advantageous for all those plants in which the combustion of fossil fuel or substances containing carbon is carried out: energy sector, metallurgical industry, cement production, etc. Relevant emissions are also present during the extraction of natural gas (Olah, et al., 2009). Excluding processes still under development (i.e. chemical looping combustion), three approaches are possible: upstream of the combustion (*pre-combustion capture*), downstream (*post-combustion capture*) or inside it, employing O₂ as the oxidizing agent (*oxy-fuel combustion*). Moreover, the techniques can be based on chemical absorption (*absorption*), or physical absorption (*adsorption*), or the permeability of a material with respect to the CO₂ (*membrane*), or the difference between the condensation or liquefaction points of the gaseous mixture's constituents (Huaman & Lourenco, 2015; Leung, et al., 2014). The capture can be part of a procedure of:

- *CCS (Carbon Capture and Sequestration)*: by a system of tubes, the carbon dioxide is sent to a storage site (generally, an underground tank). However, this solution implies an *energy penalty*: to obtain, as the output of the plant, the same quantity of useful energy, a bigger input of fuel is needed (10-40%). This means a decrease of plant's global efficiency and an increase in the amount of pollutants produced by the combustion. Moreover, the sequestration is characterized by very high costs, both capital (selection of a site suitable for the storage, realization of the needed infrastructure, installation of leakage prevention system, etc.) and operational (Atsonios, et al., 2016; contributors, 2018; Ritchie & Roser, 2017);
- *CCU (Carbon Capture and Utilization)*: the aim of this kind of procedures is not only the maintenance of the existing situation, but the conversion of an impacting by-product in a resource. Some of the most common uses of the CO₂ are (Atsonios, et al., 2016; Olah, et al., 2009; Pérez-Forte, et al., 2016; Raudaskoski, et al., 2009; Saiedi, et al., 2014):
 - *Without modification*: it can be used as the refrigerant in a CO₂ cycle, or as “gaseous piston” in *Enhanced Oil Recovery (EOR)* and *Enhanced Gas Recovery (EGR)*, or in firefighting systems, or as a solvent, etc.;
 - *As reactant to produce*:
 - *Fuels*: methane and kerosene;
 - *Chemicals*: mainly urea, but also salicylic acid, polycarbonates and inorganic carbonates.

It has to be considered that the high stability of CO₂ molecule makes it difficult to transform it by a chemical reaction.

1.2. Methanol economy as a possible solution

Considering the actual context, an interesting way is the Methanol Economy suggested by (Olah, et al., 2009). The *Methanol Economy* is intended as an economic system in which methanol (CH₃OH, usually abbreviated as “MeOH”) takes the place of fossil fuels as the main energy source and raw material for the realization of most of the substances and materials actually used. According to (Olah, et al., 2009), the basis of this economy must be the production of MeOH not from natural gas by reforming and hydrogenation of the obtained CO (industrial method for the production of methanol), but using atmospheric or industrial CO₂ (according to a CCU approach) and H₂ as feedstocks. The necessary energy input could be provided by the renewable or nuclear source, but also by fossil fuels (no longer main actors in the energy-production context, but secondary ones). The connection point between methanol production and utilization would be its easy storage and transport: according to the properties of this compound (listed in Table 1.1), this substance:

- is liquid, at atmospheric pressure, in a wide range of temperature around the atmospheric one;
- bears well high pressure (it has a high-octane number);
- does not take fire easily without a primer (it has a high auto-ignition temperature).

Lastly, such a kind of economy would cause a reduction in the emission of several pollutants generally associated with fossil fuels, like nitrogen and sulphur oxides and particulates (Methanex, 2015). Resuming, the methanol economy would generate a closed, or even negative, balance of carbon dioxide, reducing or eliminating (if it were convenient) the burden on non-renewable sources and increasing the integration of renewables (Olah, et al., 2009); furthermore, positive results would be obtained also in relation to other substances, which are harmful to the environment.

Table 1.1: Methanol's physical properties (Methanol Institute, n.d.)

| | | | |
|---|---|---|--|
| <i>Molecular Weight</i> [g/mol] | <i>Critical Temperature</i> [°C] | <i>Critical Pressure</i> [atm] | <i>Freezing Point (at 1 atm)</i> [°C] |
| 32.04 | 239 | 78.5 | -97.6 |
| <i>Boiling Point (at 1 atm)</i> [°C] | <i>Latent Heat of Vaporization (at 25 °C)</i> [kJ/mol] | <i>Latent Heat of Vaporization (at 64.6 °C)</i> [kJ/mol] | <i>Vapour Pressure (at 25 °C)</i> [atm] |
| 64.6 | 37.43 | 35.21 | 0.1674 |
| <i>Reid Vapour Pressure (defined at 37.8 °C)</i> [atm] | <i>Lower Heating Value (at 25 °C and 1 atm)</i> [kJ/mol] | <i>Higher Heating Value (at 25°C and 1 atm)</i> [kJ/mol] | <i>Auto Ignition Temperature</i> [°C] |
| 0.3158 | 638.1 | 726.1 | 470 |
| <i>LFL</i> [%] | <i>UFL</i> [%] | <i>FP (closed vessel)</i> [°C] | <i>FP (open vessel)</i> [°C] |
| 6.0 | 35.5 | 12 | 15.6 |

In the introduced economic system, methanol would be used as:

- *raw material*: the coexistence of carbon, hydrogen and oxygen in its molecular structure makes MeOH particularly versatile as a basic substance for the production of other compounds. Firstly, by a dehydration process, it is possible to generate dimethyl ether (CH₃OCH₃, usually referred to as “DME”) from methanol. At ambient temperature and pressure, DME is a gas; however, it is generally

liquefied by pressure, making it easily transportable. From DME it is possible to obtain, by further dehydrations, ethylene and propylene and, from them, plastics (polyethylene and polypropylene) and hydrocarbons. The process $\text{MeOH} \rightarrow \text{DME} \rightarrow \text{ethylene / propylene}$ is called Methanol to Olefins (Olah, et al., 2009);

- *energy source*: it can be used both for stationary power generation and mobility (automotive and naval sectors). Considering energetic purposes, there are essentially two ways of utilization:

- *combustion*: in the field of power generation, Diesel is traditionally used to meet the demand for geographical areas that are difficult to reach and/or not served by the gas network (islands, mountain areas, etc.). Diesel plants can be transformed in bi-fuels ones by operations that are feasible from both an economic and a technical point of view (Methanex, 2015). In the other important field, the automotive one, the main fossil fuels competing with MeOH are gasoline and Diesel. A comparison between the antagonists is provided in Table 1.2: firstly, it should be noticed that traditional fuels have heating value more than two times greater than methanol's one (Olah, et al., 2009). However, thanks to the contained oxygen, MeOH's stoichiometric combustion air is less than a half of that of the fossil fuels. Thus, the stoichiometric mixtures of the three fuels allow obtaining very similar quantities of energy (about 3.048, 3.048 and 2.931 MJ/kg_{air} for methanol, gasoline and Diesel respectively) (Ferrari, 2016). However, spark ignition engines and spontaneous ignition ones have very different necessities: an ICE requires a fuel with high anti-detonating properties (high octane number, NO) while a Diesel needs a fuel that can be easily ignited by the compressed air temperature (high cetane number, NC). For this reason, the principal use of methanol in the automotive sector is the feeding of spark ignition engine (Ferrari, 2016; Methanex, 2015; Olah, et al., 2009; Zhen & Wang, 2015); regarding combustion, with respect to gasoline, methanol has the following advantages (Ferrari, 2016; Methanex, 2015; Olah, et al., 2009; Yanju, et al., 2008; Zhen & Wang, 2015):

- *a greater Octane Number*, allowing to perform a deeper compression of the air-fuel mixture without knocking;
- *a higher latent heat of evaporation*, which determines a minor evaporation of the fresh mixture during the suction phase, due to the heat transfer with the tubes; in this way, it is possible to introduce a greater quantity of mixture, obtaining a bigger energy during the combustion;
- *a greater flame speed*, reducing the necessary advance of the timing of the spark.

However, it shows a relevant disadvantage, that is the *difficult cold start*, due to the combination of a *low volatility*, (expressed by a high evaporation point, a great heat of evaporation and a small Reid vapor pressure³) and a high *flash point*. Therefore, the use of methanol improves the performances of an ICE (efficiency and fuel use), but gives problems at the start (Ferrari, 2016; Yanju, et al., 2008; Zhen & Wang, 2015). Considering these aspects (and others, which will be immediately shown), the MeOH can be used in the

³ Pressure of the vapour in equilibrium with the liquid, at 37.8 °C, inside a standard tank (Treccani, s.d.).

following ways (Giacosa, 2000; Methanex, 2015; Olah, et al., 2009; Yanju, et al., 2008; Zhen & Wang, 2015):

- *pure methanol*: in this case, it is necessary to solve the problem of the cold start. Moreover, the MeOH is aggressive towards certain materials (plastic materials, elastomers, some metals); considering the high quantity of processed methanol, it is needed to provide the feeding system of a protective coating;
- *methanol/gasoline mixture (denominated with the expression M#, where # represents the volume percentage of MeOH)*: the mixing allows to solve the problem of the start, thanks to the gasoline's volatility. M<15-20 mixtures can be employed in traditional engines without modifications. Higher concentrations require modifications of the engine or Flexible Fuel Vehicles; moreover, it is necessary to add substances able to prevent the separation of MeOH from the mixture.

Instead, in spontaneous ignition engine, the traditional fuel cannot be substituted by MeOH, but by DME, whose Cetane Number is higher than Diesel's one (Olah, et al., 2009; Zhen & Wang, 2015).

Table 1.2: Comparison of MeOH, gasoline, Diesel and DME (CAMEO chemicals, s.d.; Methanol Institute, n.d.; National Center for Biotechnology Information, s.d.; Zhen & Wang, 2015)

| PROPERTIES | SUBSTANCES | | | |
|-------------------------------------|--------------------|----------|---------|----------------------------------|
| | Methanol | Gasoline | Diesel | Dimethyl ether |
| Formula | CH ₃ OH | C5-12 | C10-26 | CH ₃ OCH ₃ |
| Freezing point [°C] | -97.6 | -57 | -1/-4 | -141.5 |
| Boiling point [°C] | 64.6 | 30/220 | 175/360 | -25.1 |
| Flash point [°C] | 12 | -45 | 55 | - |
| Auto-ignition temperature [°C] | 470 | 228/470 | 220/260 | 235 |
| Lower Heating Value [MJ/kg] | 19.92 | 44.5 | 42.5 | 27.6 |
| Stoichiometric air/fuel ratio | 6.45 | 14.6 | 14.5 | 9.0 |
| Research Octane Number | 108.7 | 80/98 | - | - |
| Motor Octane Number | 88.6 | 81/84 | - | - |
| Cetane Number | 3 | 0/10 | 40/55 | 55/60 |
| Lower Flammability Level [%] | 6.00 | 1.47 | 1.85 | 2.00 |
| Upper Flammability Level [%] | 35.50 | 7.60 | 8.20 | 50.00 |
| Latent Heat of Vaporization [kJ/kg] | 1099 | 310 | 270 | 460 |

- *Electrochemical conversion* (Joghee, et al., 2015): the MeOH's oxidation can be done not only by the traditional thermochemical way (combustion), but also by the electrochemical one, by means of the so-called Direct Methanol Fuel Cell. The most suitable fields of application are electronics and mobility. In the first field, the elevated specific energetic density (about ten times the Ion-Li batteries' one) has attracted the attention of the producers of portables devices. Currently, this kind of fuel cell is sufficiently mature to enter the electronics' market. Instead, in the mobility field, the level of development is not yet sufficiently elevated, and the producers still prefer hydrogen-powered PEMFCs. The orientation of the transport sector towards the fuel cells derives from the need to reduce its environmental impact. The hydrogen PEMFCs allow this to be achieved, also obtaining a better exploitation of the fuel compared to traditional engines (30-90%). However, some problems are linked to the use of H₂:
 - *refuelling*: currently, it does not exist a system of stations of distribution, and its realization would be very expensive;
 - *on-board storing*: due to its low energetic density, it would be necessary a much bigger tank than that of traditional cars.

Methanol appears to be far more suitable:

- its bigger energetic densities (both in mass and volume terms) allow to have smaller tanks;
- the cost per unit of energy is smaller than that of hydrogen;
- the tradition fuels' infrastructure can be converted to methanol by reasonable interventions;
- it allows a more gradual conversion of the sector: according to the creator of the concept of Methanol Economy, Olah, the passage from tradition vehicles to DMFC-based ones should have some intermediate steps in terms of increasing MeOH content in the mixture.

However, DMFC's performances (efficiency, power density) are lower and costs are bigger with respect to hydrogen PEMFC's. Thus, it is necessary to continue the research regarding this kind of fuel cell.

2. CO₂ Hydrogenation: from resources to methanol

The analysed process is part of the decarbonization approach described above: the carbon dioxide, which has been removed from a gaseous flow characterized by a high content of this substances, is mixed with hydrogen, obtained by electrolysis from water (the choice of the electrochemical way to produce H₂ will be explained later). The generated mixture is sent to a reactor, in which the CO₂ hydrogenation is performed. The outputs of this process are methanol (the useful product) and water (which could be re-sent to the electrolyser).

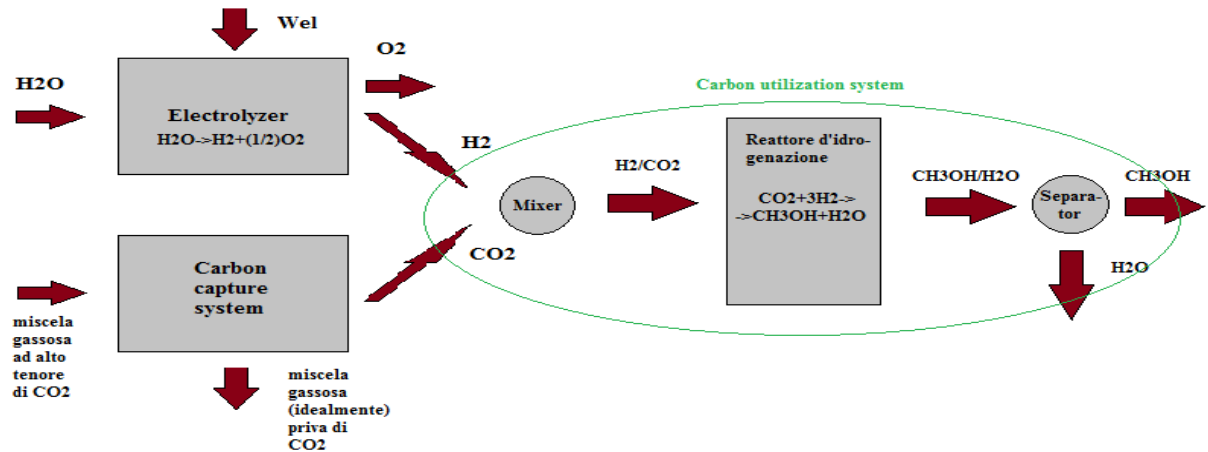


Figure 2.1: Conceptual scheme of the analysed process

2.1. H₂ production

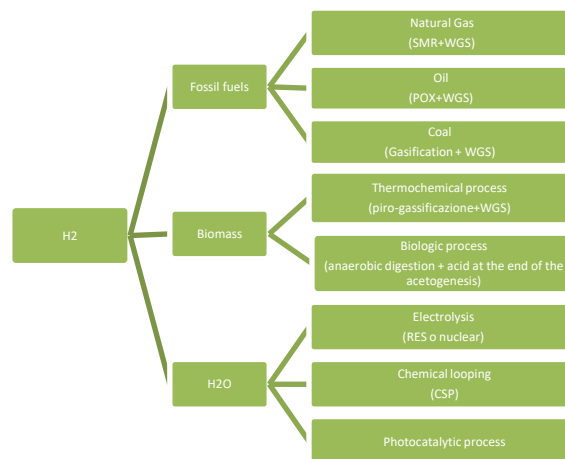


Figure 2.2: Methods to produce H₂

In Figure 2.2, the principal methods of production of H₂ currently available are resumed. The starting substance can be (Jadhava, et al., 2014):

- *fossil fuels*: the most used is natural gas, since Steam Methane Reforming ($CH_4 + H_2O \rightarrow CO + 3H_2$) requires a much shorter time than oil's partial oxidation or coal's gasification. Anyway, the resulting gas mixture is rich in CO and poor of H₂. Despite the following step of Water Gas Shift ($CO + H_2O \rightarrow CO_2 + H_2$), the obtained syngas is characterized by a too low hydrogen content; for

this reason, a cleaning section for the removal of the other substances (principally, carbon dioxide) is required. In conclusion, the way of production of hydrogen here considered has the following drawbacks:

1. the consumption of already lacking fossil fuels;
 2. a low hydrogen selectivity;
 3. the formation of a further quantity of carbon dioxide (as successively explained, during CO₂ hydrogenation, will be required 3 moles of H₂ per each mole of CO₂ and then the carbon dioxide produced here is in excess, implying the necessity of sequestration or emission in the atmosphere);
- *biomass*: both the process of biomass conversion (thermochemical and biological) are very articulated and long-lasting. Moreover, also the biomass conversion shows the drawbacks 2 and 3 of the list of the fossil fuels: both in case of pyrolysis followed by WGS (thermochemical process) and of anaerobic digestion (biological process), the produced syngas requires a *cleaning up*, to separate hydrogen from carbon dioxide and other undesired products;
 - *water*: it is possible to split the molecule of H₂O ($H_2O \rightarrow H_2 + \frac{1}{2}O_2$) through three ways:
 1. *electrolysis (electrochemical method)*: the splitting of the water molecule is forced by means of a feeding of electric power. In the optic of a decarbonization, this electricity should be derived from a renewable source or from nuclear. The most mature kind of electrolyser is the alkaline one, even if it is less efficient than PEMEC and SOEC;
 2. *chemical looping (thermochemical method)*: this technique is based on the combination of a metal characterized by two (or more) oxidation states and concentrated solar power (that is, high-temperature energy). In a first reactor, the metal, in the most oxidized state, subsides an endothermic reduction using the heat derived from CSP; pure oxygen is extracted from this component. The reduced metal is then cooled and sent in a second reactor, where it undergoes an exothermic oxidation by the introduction of water (the oxidizing agent); this second step produces the wanted hydrogen. The most mature solutions are the ZnO, S-I and Cu-Cl based. The production by chemical looping shows two drawbacks:
 - Due to the employment of high-temperature heat ($T_{rid, ZnO} = 2000$ °C), the plant has to be constructed using high performances materials;
 - The needed infrastructure is very expensive and complicated.
 3. *photocatalytic conversion*: this technology is based on the use of an electrochemical cell, in which water (which acts as electrolyte) is placed between two peculiar electrodes: the *anode* is made of a *semiconductor material*; the *cathode* is represented by the so-called *counter electrode*. Unlike the traditional electrolysis, in this case, the energy input is not an electrical power supplied to the cell, but the photons of the solar radiation on the anode (therefore, energy at low temperature). By means of this form of energy, some electrons located in the valence band of the semiconductor are excited, allowing its passage to the conduction one. The energy gap between the two bands is small enough to allow this transition, but also big enough to avoid an immediate restoration of the minimum energy

configuration. This charge separation produces a potential difference, which causes the flow of the electrons towards the cathode. They are used on the counter electrode for the formation of hydrogen from hydrons (reaction “b”), generated by the splitting of the water molecule into the electrolyte (reaction “a”). This technology is very promising in the optic of a decarbonization, but not enough mature to be employed at the industrial level.



Considering the features of the listed technologies and the purposes at the basis of the CO₂ hydrogenation, the electrolysis by alkaline electrolyser appears to be the most suitable solution. Hence, the hydrogen production section can be conceptually represented as in Figure 2.3. The electrochemical cell can be fed by RES, as prescribed by the concept of Methanol Economy. One aspect to be considered with these energy sources is the high variability over time. Since many components installed downstream the electrolyser (i.e. those in the CO₂ utilization part of the plant) are less efficient at partial loads, during the design phase it is necessary to insert a section of hydrogen compression and accumulation. A similar provision is desirable for the oxygen obtained as a secondary product: it is possible to take advantage of the gains deriving from the sale of O₂ to compensate, at least in part, the costs of the plant (Atsonios, et al., 2016).

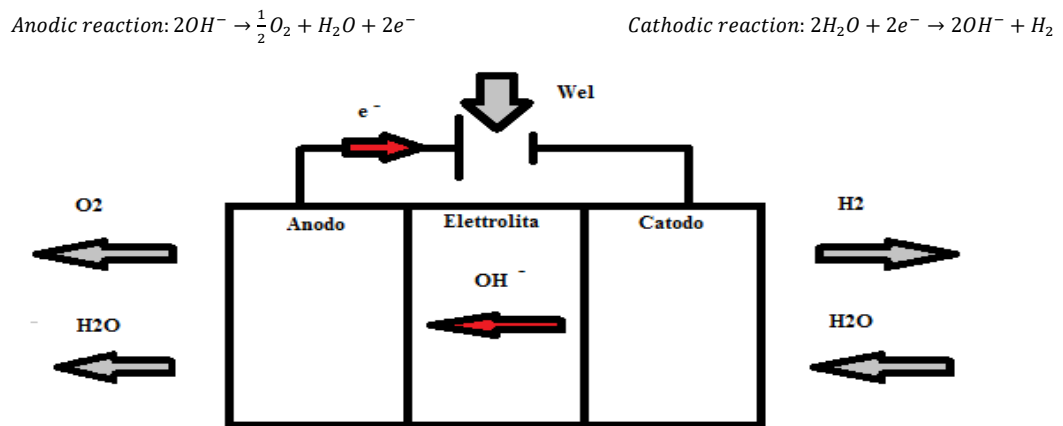


Figure 2.3: Electrolyser

2.2. CO₂ capture

As anticipated in the introductory paragraph of this chapter, the phenomenon here considered is aimed at processing fumes characterized by a high content of carbon dioxide. It is necessary to identify the most suitable mode of capture, considering that the CO₂ content is high when compared to that of the atmosphere, but low in general (in the case of coal-firing or natural gas-firing plants, the carbon dioxide concentrations are of the order of 7-14% and 4% respectively) (Leung, et al., 2014). The adoption of the post-combustion capture is the most reasonable choice, as it has already been extensively studied and used; moreover, although less efficient

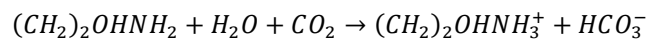
than other options, it has the following advantages (deriving from its *end of pipe approach*, (Huaman & Lourenco, 2015)):

- it makes the CO₂ hydrogenation applicable to both existing and new plants;
- being the CO₂ capture system separated from that of generation, a failure in the first one does not affect the second one (it is enough to bypass the removal section).

The chemical absorption is the most mature among the post-combustion techniques, despite it requires a scaling to be suitable to the big flows characterizing many of the applications of interest (Huaman & Lourenco, 2015; Leung, et al., 2014). Focusing on the solvent, the state of art uses an *aqueous solution (about 30%) of MonoEthanolAmine (MEA, (CH₂)₂OHNH₂)* and reaches a removal efficiency greater than 90%. However, the disadvantages related to the use of the amines are (Huaman & Lourenco, 2015; Leung, et al., 2014):

- high energy requirement to perform CO₂ desorption;
- deterioration of the amines, with consequent formation of volatile and corrosive substances and diminution of solvent efficacy.

The CO₂ capture section is conceptually represented in Figure 2.1. The CO₂-rich gaseous mixture is sent to a reactor called *scrubber*, where it encounters the solvent, producing the absorption reaction:



The “cleaned” flue gas is sent to eventual post-processing sections; indeed, the “dirty” solvent is regenerated: the CO₂ desorption is obtained by a procedure in which the solvent is firstly pre-heated by heat exchange with the clean solvent returning to the scrubber; then it is heated in a second reactor called *stripper*. The heat supplied to the stripper is generally obtained from the plant in which the fumes are processed (for example, in the case of a cogeneration plant, by operating a steam spill from the Rankine cycle turbine). High degrees of purity of the solvent and of the carbon dioxide are obtained by means of a heater and a cooler respectively. Before being immitted in the scrubber, the clean solvent undergoes a further cooling (Atsonios, et al., 2016; Huaman & Lourenco, 2015; Leung, et al., 2014).

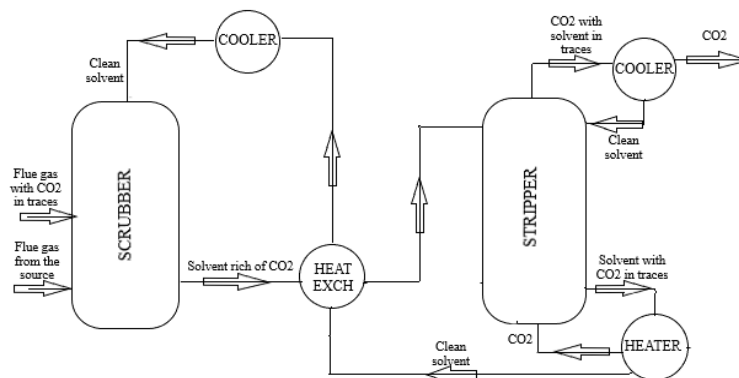


Figure 2.4: CO₂ capture section based on MEA

2.3. CO₂ hydrogenation

2.3.1. Overview

This phenomenon is the fulcrum of the plant that will be modelled later. It is constituted by the following set of reactions (Atsonios, et al., 2016; Gaikwad, et al., 2016; Lim, et al., 2009):



The reaction 1) represents the direct CO₂ hydrogenation: as anticipated, providing 3 moles of hydrogen per each mole of carbon dioxide, 1 mole of methanol and 1 mole of water are obtained. The aforesaid reaction is exothermic with a decrease in the number of moles from the reactants to the products; therefore, from the definition of Gibbs free energy and the Le Chatelier – Braun Law, it can be deduced that methanol production is favoured at low temperature and high pressure. However, not all the carbon dioxide is directly hydrogenated: a part of it is subject to reaction 2), called RWGS, which converts H₂ and CO₂ in H₂O and CO. The generated carbon monoxide undergoes a hydrogenation (reaction 3)), which leads to the formation of methanol. This reaction is exothermic (to a greater extent than the CO₂ hydrogenation, the latter being the sum of RWGS and CO hydrogenation) with a reduction in moles from the reactants to the products; therefore, also this reaction is favoured at low temperature and high pressure. In conclusion, the CO₂ hydrogenation (both the direct one and the indirect one) is globally an exothermic phenomenon.

The shown set of reaction has to be necessarily realized by the support of a catalyst. Indeed, as already mentioned, the carbon dioxide molecule is very stable. Its reactivity, and consequently its conversion, could be enhanced acting on the thermodynamic conditions, i.e. by an increase of temperature. However, being an exothermic phenomenon, the CO₂ hydrogenation does not tolerate high temperatures. Moreover, an enhancement of the reactivity does not necessarily imply an increase of the produced methanol, since many collateral reactions happen inside the reactor, producing undesired products and then not generating all the MeOH potentially obtainable (in other terms, determining a non-optimal MeOH selectivity). The principal methods of optimization of the considered process are the regulation of the thermodynamic (temperature and pressure) and of kinetic (space velocity) conditions, the use of a catalyst and the separation of reactants and products. The state of art consists of a process carried out at a temperature of 250 - 300 °C and a pressure of 5 – 10 MPa with the aid of a Cu-based catalyst (Gaikwad, et al., 2016; Jadhava, et al., 2014; Raudaskoski, et al., 2009).

2.3.2. Process tuning

2.3.2.1. Catalyst

As anticipated, the use of a catalytic substance is a necessary condition for the carbon dioxide hydrogenation. Generally, a heterogeneous catalysis is carried out: the reactants (in gaseous form) are sent into the reactor, where the catalyst (solid) is present; the latter generates the necessary conditions to the reaction (reducing its activation energy). In the case of the hydrogenation of carbon monoxide and carbon dioxide, the chemical species at the base of the catalytic phenomenon is often copper (alternatively, it is possible to use gold, silver or palladium, which are, however, more expensive) (Jadhava, et al., 2014; Liu, et al., 2003; Wang, et al., 2011). It is distributed on a *support*, on which depend the mechanical and thermal resistances of the catalyst as a whole, the acid or basic nature of the catalytic bed, the activation of the Cu and its stabilization (or, in other words, the resistance to diffusion and sintering at elevated temperatures), the mutual influence between it and the other components and the interaction with the substances involved in the catalysed reaction (Liu, et al., 2003; Natta, et al., 1978). The matrix is generally porous, in order to obtain an extended contact surface between the catalytic agent and reactants in a reactor of reasonable dimensions (Natta, et al., 1978). In the case of the phenomenon analysed here, the most suitable compounds for the realization of the support are ZnO, ZrO₂ and SiO₂ (Liu, et al., 2003). Finally, Cu is assisted (as a catalytic agent) and stabilized by substances called *promoters*. The most used promoter is Al₂O₃, but oxides of other metals can be used (Zr, Sc, Cr, B, Ga, Co and Mg) and noble metals (for example Pd, not used as the main agent due to the cost, can be used as a secondary component for H₂ cleavage) (Jadhava, et al., 2014; Liu, et al., 2003; Wang, et al., 2011).

After this review, it seems useful to enter a little in detail about the role of the materials used for the realization of the catalyst. Copper is the component which is responsible for the interaction with carbon oxides, through a phenomenon of chemical absorption; moreover, it is responsible for the homogeneous cleavage of the hydrogen molecule (Liu, et al., 2003). It has not been established with certainty whether its active phase is Cu⁰ (metallic) or Cu⁺, and this represents the major obstacle to the design of the catalyst (Liu, et al., 2003); however, a widespread interpretation is that exposed in (Lim, et al., 2009), for which Cu⁰ is responsible for the CO₂ absorption and Cu⁺ of the CO one. An aspect that has to be kept in mind is the copper's high tendency to agglomerate at process temperature; the agglomeration should be avoided as much as possible, since it would lead to larger particles of copper, with the consequences here reported (Liu, et al., 2003):

- reduction of the active surface;
- greater obstacles to the flow of the reagents to active sites.

Therefore, there would be a diminution of the activity of the catalyst. At this point, support and promoters come into play. Zinc oxide is often used as a support, since the Cu/ZnO co-presence originates what is usually called a *synergic effect*, by which ZnO improves the performances of Cu as catalytic agent, influencing its morphology (i.e. it enhances the dispersion of the copper and stabilized the dispersed particles) and activation (i.e. it increases the intrinsic activity of the copper) (Behrens, et al., 2012; Liu, et al., 2003). According to the most common interpretation, thanks to the oxygen vacancies that characterize its crystalline structure (such as Wurtzite), zinc oxide is able to heterogeneously split the hydrogen molecule (forming ZnH and OH), which then reaches the active copper sites (Cu⁰ or Cu⁺) by spillover (Liu, et al., 2003). An alternative interpretation

is that ZnO can contribute to the formation of the active phase, of Cu-Zn type (Liu, et al., 2003). Another advantage of zinc oxide is that it allows the removal (by adsorption) of any substances introduced with reagents that could poison copper (such as sulphides) (Liu, et al., 2003). A possible alternative as a support is zirconia (ZrO_2), which has a high mechanical and thermal stability, accompanied by a considerable activity (greater than those of Al_2O_3 and SiO_2) (Liu, et al., 2003). Zirconium oxide can also be used as a promoter in a Cu/ZnO/ ZrO_2 catalyst with excellent results: copper binds to oxygen derived from zirconia, producing CuO, while the remaining zirconium ions cause the Cu^+ ions generation, which is essential for the carbon monoxide hydrogenation (that is one of the main collateral products of the whole process) (Liu, et al., 2003). Silica (SiO_2) is considered interesting as a support, due to its porosity and compatibility with the thermal cycles. However, a catalytic bed supported by SiO_2 requires promoters to compensate its low activity (Liu, et al., 2003; Wang, et al., 2011). On the other hand, the aluminium oxide is generally used as a promoter, since it preserves the dispersion of the active phase (by the formation of zinc aluminate, $ZnAl_2O_4$) and promotes the interaction between the catalytic bed and carbon monoxide (Liu, et al., 2003). Another very valid promoter is Ga_2O_3 , whose presence raises the activation of copper in oxidized form (Cu^+); furthermore, another (and probably chief) advantage of gallium oxide is the small particle size (Wang, et al., 2011).

One of the most important aspects regarding the Cu-catalysed hydrogenation is the strong influence of the catalyst structure, as already told, it has to be characterized by a large Cu exposed surface (since linked by an almost linear relationship to the yield) and by a high intrinsic activity (generated by the interaction between the main catalytic agent, support and promoters). Therefore, the impact of the method adopted for the catalytic bed preparation is an aspect to be taken into account (Behrens, et al., 2012; Jadhava, et al., 2014). Co-precipitation is currently considered the best option for copper -based catalysts: the bed is obtained by sedimentation of particles of the constituents, starting from solutions which are rich of salts derived from them; this is caused by the introduction of precipitators (sodium carbonates or sodium oxalates), which are removed, after the precipitation, by means of a centrifuge or by evaporation (Behrens, et al., 2012). (Wang, et al., 2011) reports the performances (taken from literature) of various catalyst differing for composition and method of preparation; from this article, it can be deduced that very high selectivities can be obtained (over 99%), but the carbon dioxide conversion is generally low (the greatest reported value is 21%). Therefore, a $CO_2/CO/H_2$ recirculation has to be realized.

2.3.2.2. Thermodynamic parameters – kinetic parameters – catalyst combined effect

The selection of the operating set up (in terms of temperature, pressure and spatial velocity) and of the catalyst to be employed are the two complementary ways of optimization at the reactor level. As already mentioned, CO_2 hydrogenation is favoured at relatively low temperatures and high pressures; however, it is generally preferred not to use very high pressures to enhance the reaction, since they would require significant energetic and economic costs and would generate safety problems. On the other hand, to increase the spatial velocity to obtain a greater amount of methanol per unit of time is not usually a good idea: a relatively low spatial velocity allows the reactants for remaining inside the reactor for a long time and then favours their conversion. Hence, the usual approach consists in using suitable (for the process) thermodynamic and kinetic conditions and relying on an efficient catalyst to improve conversion and selectivity. However, the

optimization in terms of temperature, pressure and spatial velocity can be advantageous, as demonstrated by (Gaikwad, et al., 2016) through an experimental CO₂ hydrogenation catalysed by Cu/ZnO/Al₂O₃ with particles' size equal to 100-300 μm, at pressures belonging to the range [46;442] bar, temperatures comprised in the interval [200;300] °C and GHSV up to 100000 h⁻¹. They have confirmed the advantage of high pressures and have concluded that, at a temperature of almost 260-280 °C, both conversion and selectivity show a maximum; moreover, they have observed that, due to the condensation of water and methanol at very high pressures (in the considered range of temperature), mass transfer limitations rise and higher the spatial velocity is, greater these limitations are. In order to avoid these obstacles to the mass flow, a fine (in terms of particles' size) catalyst is required. In conclusion, a contribute to the good performances of the phenomenon can be obtained operating at high pressure, temperature close to 260-280 °C and not too high spatial velocity. However, it is not enough and both a catalyst and the recirculation of the reactants are required.

2.3.2.3. Products' separation and recycle

Even if optimal thermodynamic and kinetic conditions and a performant catalyst are used, only a not very high fraction of the carbon dioxide introduced into the reactor is converted by a single step; in order to convert the reactants as much as possible, they have to be recirculated, realizing the hydrogenation by multiple steps. However, at the outlet of the reactor, reactants and products are mixed. Hence, they have to be separated, so that reactants can be recirculated and products (methanol, water and other collateral products) can go to a further purification section. According to (Atsonios, et al., 2016; Van-Dal & Bouallou, 2013), the separation is generally carried out by two flash separators, basing on the different volatility of reactants and products. To bring the mixture to the operating conditions of the first separator, it previously passes through a cooling section. After the formation of the gaseous and liquid phases, the former is sent to the recirculation, while the latter is brought to the operating condition of the second separator by a lamination. The two obtained gaseous phases are mixed (after a compression of the second one up to the pressure of the first one) and a small amount (<1%) is removed to avoid collateral products accumulation in the reactor (which would have a negative influence on the position of the reactions' equilibria). Successively, the gas is compressed, to reach the reactor inlet pressure. After that, the recycled mixture is mixed with fresh reactants, and the whole flow is preheated to the reactor inlet temperature. The remaining liquid phase is preheated and successively divided in MeOH on one side and water on the other (here, collateral products are negligible) using a distillation column. The heat required for the preheating before the reactor and the column and for the reboiler of the column itself is taken from the cooling section.

3. Modelling of a methanol production plant implementing CO₂ hydrogenation and H₂O electrolysis

The aim of this thesis was to simulate the implementation of the CO₂ hydrogenation process within a plausible plant, in which the captured carbon dioxide was converted into methanol through hydrogen obtained by water electrolysis. To reach this goal, it was necessary to start from a thermodynamic evaluation of the hydrogenation, which provided, depending on the defined thermodynamic conditions and the feeding composition, the ideally obtained products. Successively, an assessment of the influence of the reactor on this ideal situation was needed; it was done defining a reactor-level kinetics, starting from definitions of the reactor's constructing parameters and reactions' kinetics obtained from the literature. Finally, the effects of the interaction between the hydrogenation process and the other components of the plant in which the hydrogenator was placed had to be quantified; for this purpose, the previously obtained kinetics was used to simulate the reactions.

3.1. Thermodynamic evaluation of CO₂ hydrogenation

As already mentioned, CO₂ hydrogenation is constituted by the following set of reactions:



By a strictly theoretical point of view, it has been already said that the process is globally exothermic and favoured at relatively low temperature and high pressures (according to Gibbs free energy definition and Le Chatelier – Braun Law); moreover, as analysed by (Lim, et al., 2009), the feeding composition greatly affects the methanol production. To simulate the process, a much deeper preliminary study of the effects of thermodynamics and composition had to be done, in order to fix a set of operating condition. For this reason, it was decided to consider a flow entering the reactor made of carbon dioxide and hydrogen, select a set of basic conditions (in terms of T, p and H₂/CO₂) and operate variations of them singularly taken. The selected basic conditions are reported in Table 3.1. They were taken from (Atsonios, et al., 2016); regarding the composition, it was chosen to use a stoichiometric mixture of hydrogen and carbon dioxide, as can be noticed at a glance at reaction 1) above; concerning temperature and pressure, these values are coherent to the conclusion of (Gaikwad, et al., 2016).

Table 3.1: basic operative conditions

| H ₂ /CO ₂ [-] | T [°C] | P [bar] |
|-------------------------------------|--------|---------|
| 3 | 250 | 65 |

The described procedure was applied using the software Aspen Plus®. The component at the basis of this study was a RGibbs reactor, which, given the reactants' flow and the thermodynamic conditions of the

phenomenon to be realized, determines the products and the related heat duty; to make its calculations, the component does not rely on the definition of the reactions, but looks for the composition at the outlet of the reactor minimizing the Gibbs free energy. Each selected set up was evaluated considering two aspects: on one side, the molar fractions of the involved chemical species in the products; on the other side, the performances of the process, in terms of carbon dioxide conversion, selectivity of the process towards methanol and resulting yield (Natta, et al., 1978):

$$CO_2 \text{ conversion} = \frac{\text{reacted moles of } CO_2}{\text{fed moles of } CO_2}$$

$$MeOH \text{ selectivity} = \frac{\text{produced moles of } MeOH}{\text{reacted moles of } CO_2}$$

$$MeOH \text{ yield} = \frac{\text{produced moles of } MeOH}{\text{fed moles of } CO_2} = CO_2 \text{ conversion} * MeOH \text{ selectivity}$$

Variation of the reactants' composition

In order to evaluate the effect of the reactants' composition, it was considered, at basic temperature and pressure, to have a total molar flow rate entering the reactor equal to 100 kmol/s and to vary the CO_2 molar flow rate in the range [99;1] kmol/s, obtaining the H_2 as a hundred's complement. In this way, a H_2/CO_2 varying in the interval [0.01;99], with most of the values belonging to [0.01;10], was obtained. Considering the several sources found in literature, $H_2/CO_2 > 10$ are rarely used. Consequently, it seemed reasonable to limit the analysis to the range [0.01;10]. The results are resumed in Figure 3.1 and Figure 3.2. For very low hydrogen contents, carbon dioxide seems to be unreacted and the main products are carbon monoxide and water, while methanol's molar fraction is almost null. Obviously, the equimolar RWGS is advantaged, in these conditions, with respect to CO and CO_2 hydrogenations, which require more moles of hydrogen per unit mole of carbonaceous species to occur. However, too low amounts of hydrogen also slow down this reaction. Consequently, low conversions, selectivities and yields are obtained. An increase in the number of moles of hydrogen per unit mole of carbon dioxide allows the production of methanol by the two hydrogenations. This results in an increase of the molar fractions of methanol and water (which become similar) and a decrease of the CO's one (which tends progressively to zero). In particular, the H_2O 's molar fraction reaches its maximum at a $H_2/CO_2 \sim 2.5$, while MeOH's one at a $H_2/CO_2 \sim 3.5$. Consequently, better performances are obtained. In particular, the selectivity shows a fast growth, which starts to saturate in correspondence of the maximum of the water's molar fraction.

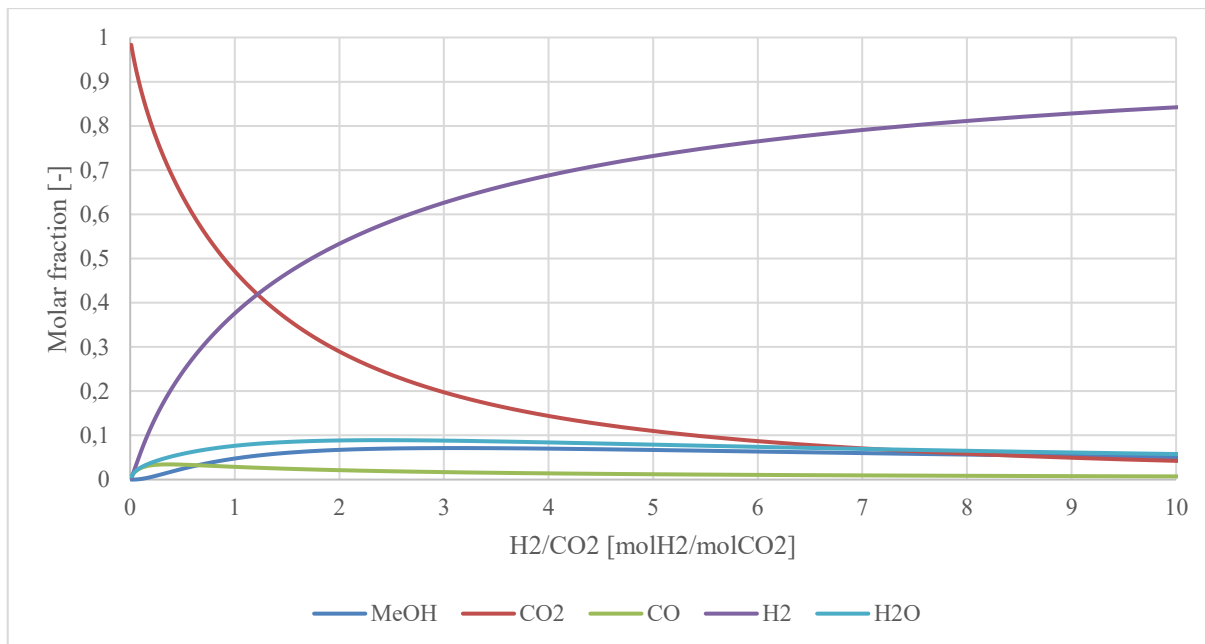


Figure 3.1: Products' composition VS H₂/CO₂

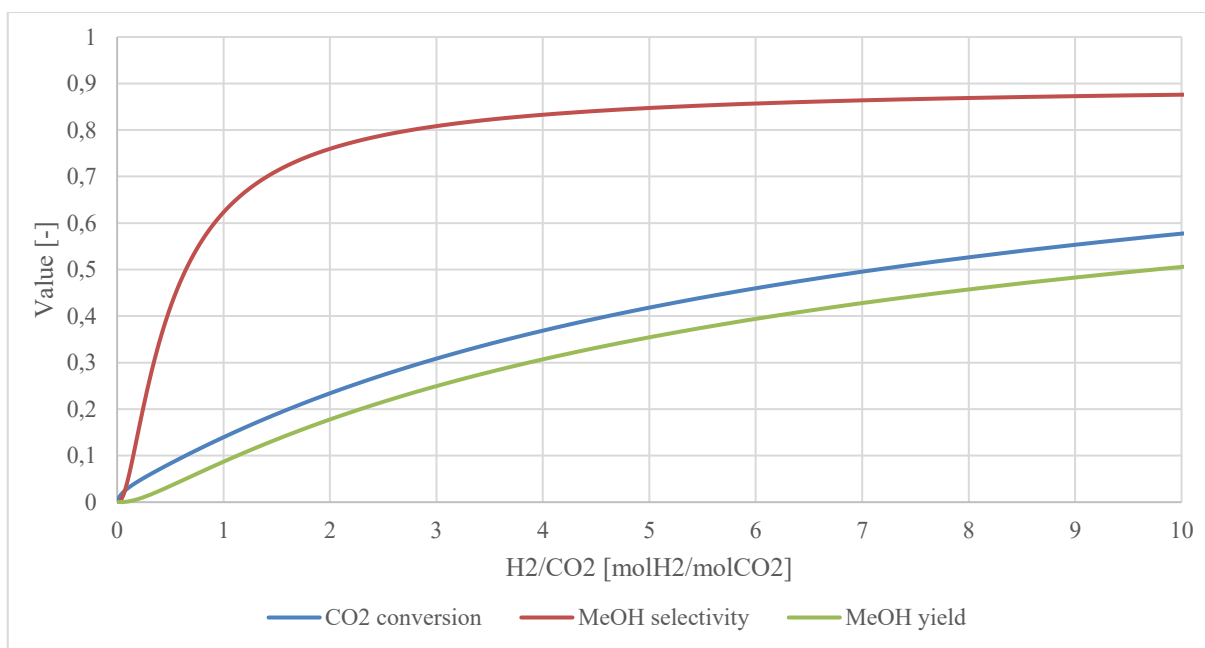


Figure 3.2: Performances VS H₂/CO₂

Variation of the temperature

The evaluation of the influence of temperature on the process was done fixing the feeding (a stoichiometric mixture with a total flow rate equal to 100 kmol/s) and the pressure (equal to the basic one) and operating a variation of the temperature in the range [100;500] °C. However, according to literature, the interval can be restricted to [200;300]: on one side, temperatures below 200 °C are rarely used, since they determine a low activity of the catalyst; on the other side, values bigger than 300° determines a phenomenon of sintering of the catalyst and consequently a reduction of the exposed active surface and of the activity of the catalytic bed. Hence, it has been decided to consider the restricted range. The results are resumed in Figure 3.3 and Figure 3.4. At T=200 °C, it can be seen that water and methanol's molar fractions assume their maximum values, which are equal one to each other, while carbon monoxide is almost absent; this means that the low temperature favours the exothermic CO₂ hydrogenation, leading to the production of MeOH and H₂O, and inhibits the endothermic RWGS, which is the starting step of the indirect process. As expected, an increase of temperature enhances the CO₂ conversion to CO, while inhibits the hydrogenations. As a result, the molar fractions of methanol and water diminish, while the CO's one increase; water's fraction decreases less than methanol's one (since the diminished production from CO₂ hydrogenation is compensated by the increased quantity resulting from RWGS) and reaches its minimum at T=300 °C. All the described processes result in decreasing performances with temperature (as expected). In particular, also the conversion reaches its minimum at T=300 °C.

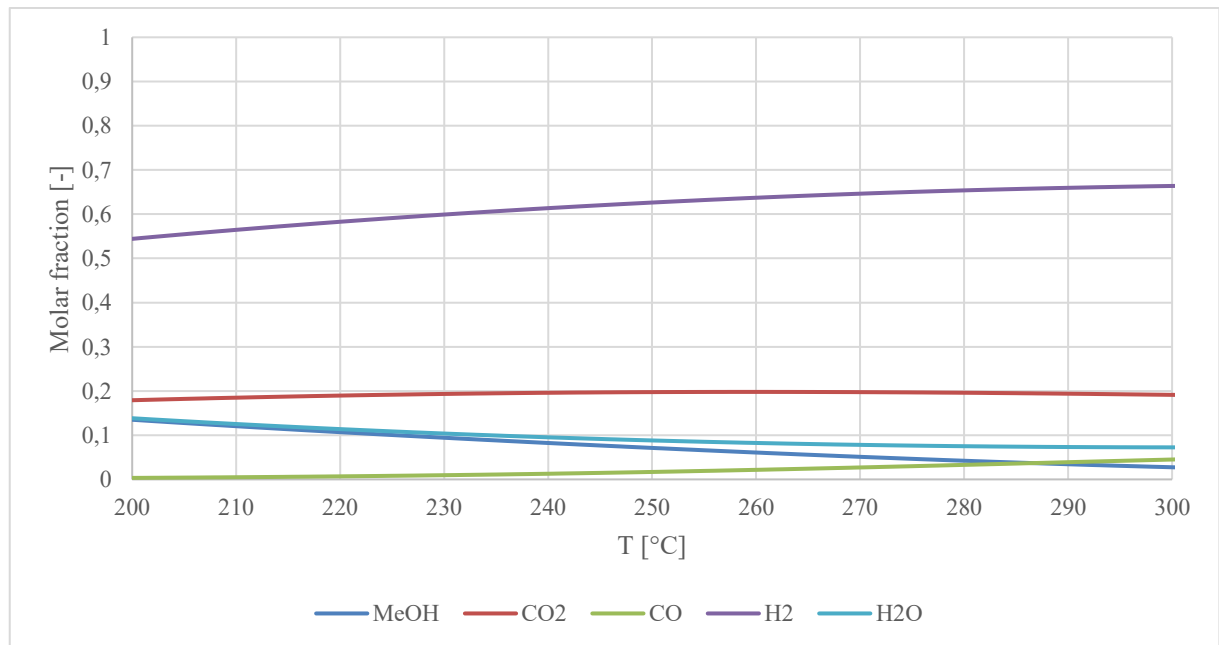


Figure 3.3: Products' composition VS temperature

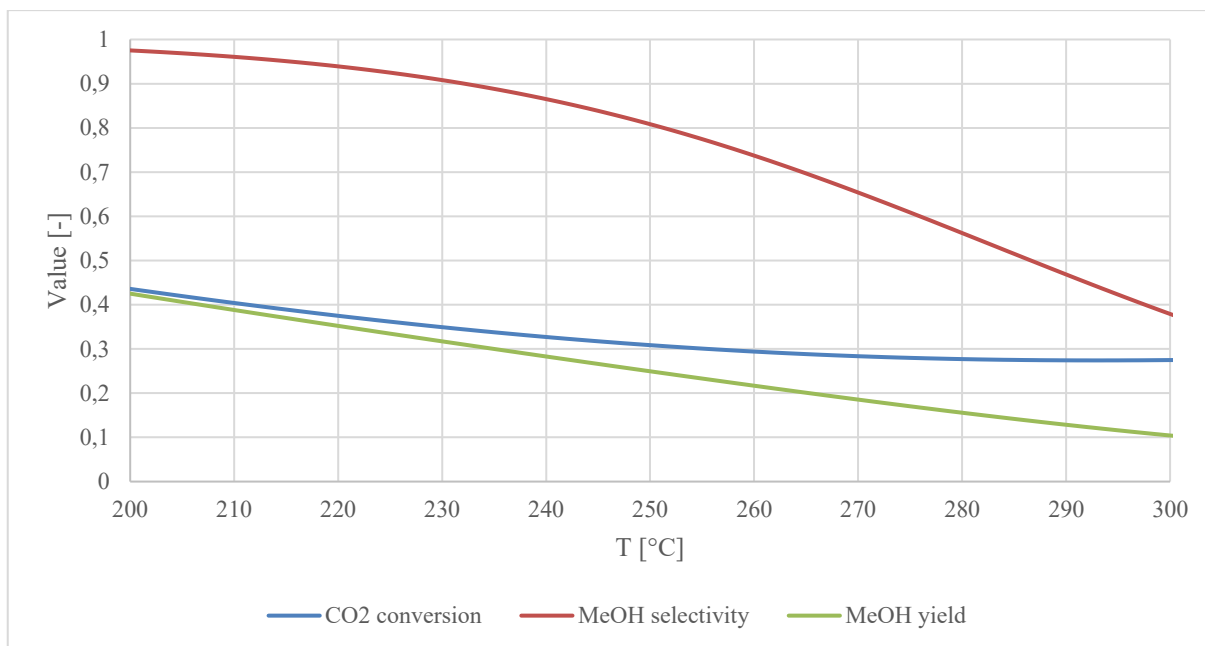


Figure 3.4: Performances VS temperature

Variation of the pressure

The influence of the pressure on the process was assessed fixing the feeding (a stoichiometric mixture with a total flow rate equal to 100 kmol/s) and the temperature (equal to the basic one) and considering a variation range equal to [50;100] bar (according to the literature, most of the applications of CO₂ hydrogenation falls in this interval). The results are shown in Figure 3.5 and Figure 3.6. They are fully coherent to what Le Chatelier – Braun Law says: when considering spontaneous reactions with decreasing number of moles passing from the reactants to the products, performed at high pressure, the equilibrium is shifted towards products (in the direction of moles diminution). In the considered case, the two hydrogenations are enhanced by the high pressure, while the RWGS is not influenced by it. For this reason, the higher is the pressure, the higher are methanol and water's molar fractions. In particular, the former is smaller than the latter up to pressures close to 100 bar, where they become equal: it is required a high pressure to produce, by the two hydrogenations, an amount of methanol equal to the amount of water produced by CO₂ hydrogenation and RWGS. Because of what it has been said up to here, an increase in pressure has a good effect on the performances of the process.

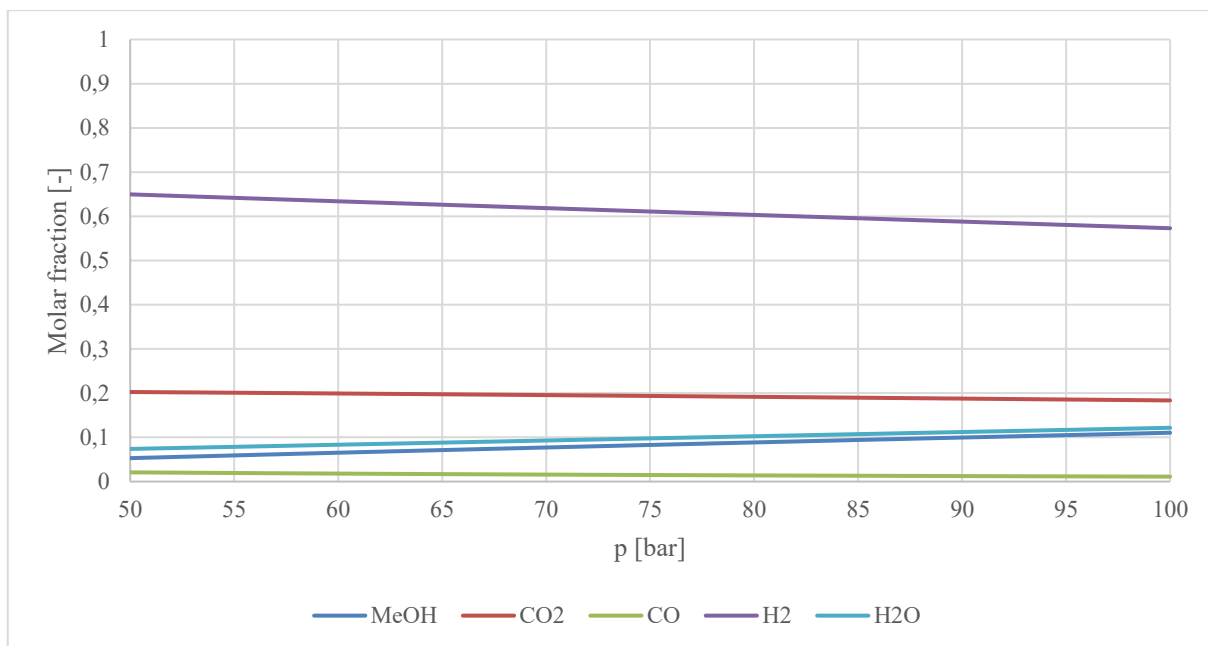


Figure 3.5: Products' composition VS pressure

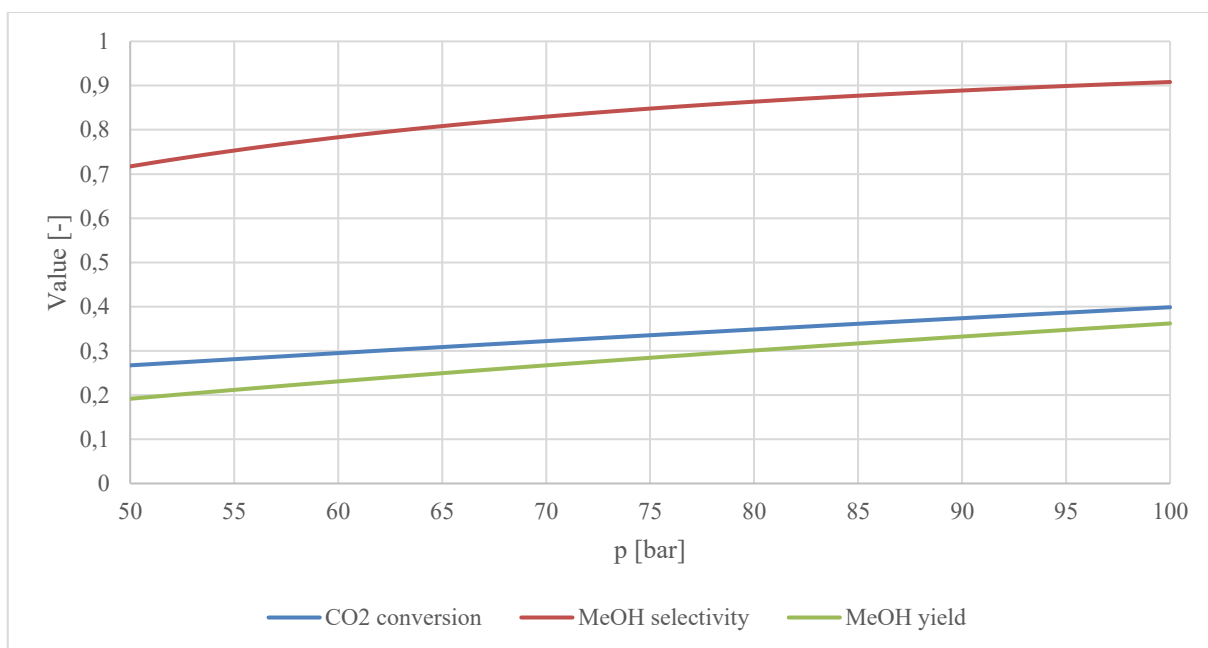


Figure 3.6: Performances VS pressure

Conclusions about thermodynamics

Basing on the made calculations, it can be concluded that, at the basic conditions, a CO₂ conversion of the 31%, a selectivity of the process with respect to methanol equal to 81% and a yield of the 25% are obtained. Considering the graphs above and the relative comments, these basic conditions do not appear as the best one: it seems that a temperature decrease and a pressure increase would be beneficial. However, as already mentioned, it has to be remembered that a too low T does not allow the activation of the catalyst, while a too high p implies relevant energetic and economic cost. Considering all these facts, it was decided to use the set up taken from (Atsonios, et al., 2016) for the following analysis.

3.2. Study of CO₂ hydrogenation at reactor level

In the previous study, the behaviour of the process was assessed considering only thermodynamic phenomena. However, that is an ideal situation. It has to be taken into account that the analysed set of reactions occurs thanks to the presence of a catalyst. In this thesis, it was considered to perform a heterogeneous catalysis, which is characterized by the following consecutive processes (Froment, et al., 2010):

1. Diffusion of reactants from the main flow to the surface of a pellet of the catalyst;
2. Diffusion of reactants through the pores of the pellet;
3. Adsorption of reactants on the active surface;
4. Diffusion of adsorbed species on the surface and reaction;
5. Desorption of products;
6. Diffusion of products through the pores of the pellet;
7. Diffusion of products from the surface of the pellet to the main flow.

Each one of these phases is characterized by its velocity, which affects not only the phase itself, but the entire process: a typical comparison made when evaluating the performances of a catalytic reactor is that between the rate of diffusion of the chemical species through the porous catalyst and the rate of reaction of the species themselves. All these kinetic factors limit the performances that could be obtained according to thermodynamics. For this reason, in order to simulate a plant containing a CO₂ hydrogenator, it is necessary a reactor kinetic scheme, which combines thermodynamics and kinetics. In this thesis, it was done in two steps:

1. Simulation of the reactions participating to CO₂ hydrogenation;
2. Definition of a power-law kinetic scheme.

3.2.1. Simulation of the reactions participating to CO₂ hydrogenation

The aim of this step was to simulate the reactions of interest at the reactor level and collect data regarding their outputs, which would be used, in the following step, as a base of a fitting procedure to obtain the kinetic parameters. Successively, the defined kinetics would be implemented in Aspen Plus[®], on which the simulation of the recycles is not too difficult. Since the scheme would be used in Aspen Plus[®], which requires to define the reactions constituting the set one by one, each reaction was singularly considered. The power-law form was selected for its simplicity and compatibility with the simulation software.

3.2.1.1. Model definition

The assumptions at the base of this preliminary simulation of the reactor were:

1. *mono-tubular reactor*;
2. *plug flow reactor*: this implied that:
 - (a) the phenomenon of axial dispersion could be ignored, since it was negligible with respect to the plug flow;
 - (b) the radial gradient of the physical quantities could be considered null;
3. *isobaric reactor*: pressure drops can be directly evaluated in Aspen Plus[®] and, as it will be seen in the plant simulation, they are generally small;
4. *isothermal reactor*: it is an existing technology and can be easily modelled in Aspen Plus[®]; moreover, this implied also isothermal pellets, which was a very simplifying hypothesis;
5. *packed bed catalyst* (the features of which will be shown in a subsequent paragraph) *made of spherical pellets having a diameter which was uniform along the reactor and much smaller than the tube one*;
6. *stationary conditions*;
7. *chemical species in the gaseous state and approximated as ideal gasses*;
8. *uniform physical properties of the fluid in each axial section of the tube*.

According to the hypothesis, the reactor was approximated by one-dimensional axial heterogeneous steady-state model: the main equation was the continuity one applied to the fluid phase, while the same equation applied to a single pellet was considered as a boundary condition in each axial section of the reactor; also the pellet was approximated as one-dimensional, but in the radial direction. Basing on these considerations, the reactor model was constructed considering the following equations:

- *Fluid phase (gas flow going through the reactor)*

$$-u_f \frac{dC_j}{dz} = k_{g,j} a_v (C_j - C_{j,s}^s) \quad (E1)$$

- *Solid phase (pellet of catalyst)*

$$\frac{D_{eff,j}}{r^2} \frac{\partial}{\partial r} \left(r^2 \frac{\partial C_{j,s}}{\partial r} \right) + \sum_i^{nr} \nu_{j,i} \rho_p r_{i,mc} = 0 \quad (E2)$$

- *Boundary conditions*

$$C_j = C_{j,0} \quad z = 0 \quad (\text{B1})$$

$$k_{g,j} a_v (C_j - C_{j,s}^s) = -D_{eff,j} \frac{\partial C_{j,s}}{\partial r} \quad r = \frac{D_p}{2} \quad (\text{B2})$$

$$\frac{\partial C_{j,s}}{\partial r} = 0 \quad r = 0 \quad (\text{B3})$$

Where

- u_f is the velocity of the main fluid [m_f/s];
- C_j is the concentration of the chemical specie j [mol_j/m^3];
- z is the axial coordinate along the tube [m_r];
- $k_{g,j}$ is a coefficient which takes into account the transport limitations that the chemical specie j has to overcome to reach the surface of a pellet [$\text{m}^3/(\text{m}^2 \cdot \text{s})$];
- a_v is the surface of a pellet per unit of volume of the reactor, defined as $a_v = a_p(1 - \varepsilon_b)$ [m^2/m^3];
- a_p is the pellet surface per unit of volume, defined as $a_p = \frac{4\pi R_p^2}{\frac{4}{3}\pi R_p^3} = \frac{3}{R_p}$ [m^2/m^3];
- R_p and D_p are the radius and the diameter of the pellet [m];
- ε_b is the void fraction of the catalytic bed [-];
- $C_{j,s}^s$ is the concentration of the chemical specie j on the surface of the pellet [mol_j/m^3];
- $D_{eff,j}$ is the effective diffusivity of the chemical specie j inside the pellet, given by $D_{eff,j} = D_{jf} \frac{\varepsilon_p}{\tau_p}$;
- D_{jf} is the mean binary diffusivity of the chemical specie j in the gaseous mixture [m^2/s];
- ε_p is the pellet porosity [-];
- τ_p is the pellet tortuosity [-];
- r is the pellet radial coordinate [m];
- $C_{j,s}$ is the concentration of the chemical specie j inside the pellet [mol_j/m^3];
- $nr = 3$ is the number of reactions;
- $\nu_{j,i}$ is the stoichiometric coefficient of the chemical specie j in the reaction I; it is negative for reactants and positive for products;
- ρ_p is the apparent density of the pellet [$\text{kg}_{cat}/\text{m}^3$];
- $r_{i,mc}$ is the rate of the reaction i per unit of mass of catalytic material, referred to the carbonaceous reactant [$\text{mol}_{ref}/(\text{kg}_{cat}\text{s})$].

(B1) expresses the starting values of the concentrations of the chemical species, (B2) the continuity of the heat flux at the pellet interface and (B3) the symmetry of the concentration profile at the centre of the pellet.

3.2.1.2. Catalyst morphology

In the previous paragraph, there are many terms referring to the morphology of the catalytic bed. For this reason, it appears necessary to do a brief description of them. As told before, the catalyst is made of pellets of catalytic material, among which some interstices are present. Also the single pellet is not fully formed by the mentioned material, but shown a porous structure. To consider the presence of the pore inside a pellet, two quantities are defined:

- Porosity of the pellet $\rightarrow \varepsilon_p = \frac{V_{pore,p}}{V_p}$;
- Apparent density of the pellet $\rightarrow \rho_p = \frac{M_{cat,p}}{V_p}$;

which are correlated, through the density of the catalytic material ρ_{cat} , by the correlation:

$$\varepsilon_p = 1 - \frac{\rho_p}{\rho_{cat}}$$

To consider the presence of the interstices between the pellets, two other quantities are defined:

- Void fraction of the bed $\rightarrow \varepsilon_b = \frac{V_{interstices}}{V_{bed}}$;
- Bulk density of the bed $\rightarrow \rho_b = \frac{M_{cat,tot}}{V_{bed}}$;

which are correlated, through the apparent density of the pellet ρ_p , by the correlation:

$$\varepsilon_b = 1 - \frac{\rho_b}{\rho_p}$$

Finally, the tortuosity of the pellet τ_p considers that the pathway of the substances through the pores is not a straight line (Froment, et al., 2010).

3.2.1.3. Fluid physical properties

Obviously, the model had also to consider the physical properties of the fluid, which varied as the fluid flowed the reactor and its composition changed. In this thesis, three quantities had to be calculated section by section:

- *Density*: knowing the molar fractions of all the chemical substances in the considered section, it was possible to calculate their partial densities by the ideal gas equation:

$$\rho_j = 10^2 \left(\frac{p}{R_u T} \right) * (x_j MM_j)$$

Where:

- p is the total pressure [bar];
- $R_u = 8,314$ is the universal gas constant [J/(mol*K)];
- T is the temperature [K];
- x_j is the molar fraction of the chemical specie j [-];
- MM_j is the molar mass of the chemical specie j [g/mol].

Then, the global density of the fluid was found summing the partial densities;

- *Viscosity*: in order to evaluate the viscosity, it had to be taken into account that water and methanol are strongly polar substances and not all the methods for the evaluation of this quantity are suitable to deal with this kind of substances. Basing on the comparison made in (Poling, et al., 2001), it was chosen to use First Order Chapman-Enskog to evaluate the viscosity of the single chemical species:

$$\eta_j = \frac{26.69(MM_j T)^{1/2}}{\sigma_j^2 \Omega_{v,j}}$$

with the collision integral $\Omega_{v,j}$ evaluated using the Neufeld formulation (applicable if $0,3 \leq T_j^* \leq 100$):

$$\Omega_{v,j} = [A(T_j^*)^{-B}] + C[\exp(-DT_j^*)] + E[\exp(-FT_j^*)]$$

where

- $A = 1.16145$;
- $B = 0.14874$;
- $C = 0.52487$;
- $D = 0.77320$;
- $E = 2.16178$;
- $F = 2.43787$;
- $T_j^* = \frac{k}{\varepsilon_j} T$;
- $k = 1.3807 * 10^{-23}$ is the Boltzmann constant [J/K];
- σ_j and ε_j are, according to the Lennard-Jones 12-6 potential formulation, the distance between two atoms which makes the pair-potential energy to be null and the “minimum of the pair-potential energy” respectively (Poling, et al., 2001).

σ_j and $\frac{k}{\varepsilon_j}$ are tabulated for several substances in (Poling, et al., 2001).

In order to combine the partial viscosities of the ns chemical species to obtain that of the fluid, it was chosen to use the Method of Reichenberg (Poling, et al., 2001), which employs a complex system of equations. The main equation, which determines the viscosity of the mixture (made of ns components) η_m , is:

$$\eta_f = \sum_{j=1}^n K_j \left(1 + 2 \sum_{i=1}^{j-1} H_{ji} K_i + \sum_{\substack{i=1 \\ i \neq j}}^{ns} \sum_{\substack{k=1 \\ k \neq j}}^{ns} H_{ji} H_{jk} K_i K_k \right)$$

The term K_j is determined by the following expression:

$$K_j = \frac{x_j \eta_j}{x_j + \eta_j \sum_{\substack{k=1 \\ k \neq j}}^{ns} x_j H_{jk} \left[3 + \left(2 \frac{MM_k}{MM_j} \right) \right]}$$

while H_{ji} is obtained through the following equation:

$$H_{ji} = \left[\frac{MM_j MM_i}{32(MM_j + MM_i)^3} \right]^{1/2} (C_j + C_i)^2 \frac{[1 + 0.36 T_{rji} (T_{rji} - 1)]^{1/6} F_{Rji}}{(T_{rji})^{1/2}}$$

In the previous expression, there are many contributes which have to be expressed:

$$T_{rj} = \frac{T}{T_{cj}}$$

$$C_j = \frac{MM_j^{1/4}}{(\eta_j U_j)^{1/2}}$$

$$U_j = \frac{[1 + 0.36T_{rj}(T_{rj} - 1)]^{1/6} F_{Rj}}{(T_{rj})^{1/2}}$$

$$F_{Rj} = \frac{T_{rj}^{3.5} + (10\mu_{rj})^7}{T_{rj}^{3.5} + [1 + (10\mu_{rj})^7]}$$

$$\mu_{rj} = 52.64 \frac{\mu_j^2 p_{c,j}}{T_{c,j}^2}$$

$$T_{rji} = \frac{T}{(T_{cj} T_{ci})^{1/2}}$$

$$F_{Rji} = \frac{T_{rji}^{3.5} + (10\mu_{rji})^7}{T_{rji}^{3.5} + [1 + (10\mu_{rji})^7]}$$

$$\mu_{rji} = (\mu_{rj} \mu_{ri})^{1/2}$$

As it can be seen, the method takes into account the polarity of the mixed chemical species by the corrective terms F_{Rj} and F_{Rji} , in which appear the dipole moments of the considered substances. Also the values of μ_j of several compounds are reported in (Poling, et al., 2001).

- *Diffusivity*: in the considered case, two mechanisms were relevant (He, et al., 2014):
 - *Molecular diffusion*: process which occurs when the mean free path of the molecules is much longer than the mean diameter of the pores; in other words, the pores are so wide that the collisions of the gas molecules among them are more probable than those of the particles against the walls of the pores. The relative binary diffusivities of the substances composing the mixture have been evaluated using the Method of Fuller, which appears as the most precise of the possible methods (Poling, et al., 2001):

$$D_{ji} = \frac{0.00143T^{1.75}}{pMM_{ji}^{1/2} [(\Sigma_v)_j^{1/3} + (\Sigma_v)_i^{1/3}]^2}$$

where D_{ji} is in cm^2/s , the temperature is in K, the pressure in bar, $\Sigma_{v,j}$ is the atomic diffusion volume of the chemical specie j (tabulated in (Poling, et al., 2001)) and MM_{ji} is defined in the following way:

$$MM_{ji} = 2[(1/MM_j) + (1/MM_i)]^{-1}$$

- *Knudsen diffusion*: a phenomenon that occurs when the mean free path of the gas molecules is similar to the diameter of the pore; this means, that the collisions of the particles among them

and against the walls have comparable probability. The Knudsen diffusivity of each substance has been evaluated with the following expression (He, et al., 2014):

$$D_{j,K} = \frac{d_p}{3} \sqrt{\frac{8R_u T}{\pi M M_j}}$$

where d_p is the pores' mean diameter.

To understand if the mixture, in a certain region of the catalytic bed, is affected by one of these mechanisms or both, the Knudsen number K_n is used (for $K_n \ll 0.1$ the molecular diffusion is the most important, for $K_n \gg 10$ the Knudsen diffusion is predominant). For the single chemical specie, it is evaluated with the following formula (He, et al., 2014):

$$K_{n,j} = \frac{\lambda_j}{d_p}$$

where λ_j is the mean free path of the chemical specie and is calculated with the expression below (all the quantities are in SI units of measure):

$$\lambda_j = \frac{kT}{\sqrt{2} p \pi d_{g,j}^2}$$

where $d_{g,j}$ is the effective diameter of a molecule of the specie j and can be approximated with σ_j .

To combine the binary diffusivities among them and with the Knudsen ones to obtain the mean binary diffusivity of the chemical specie j in the fluid, Blanc's law was used in case of presence of both the mechanisms:

$$D_{jf} = \left(\sum_{\substack{i=1 \\ i \neq j}}^n \frac{x_i}{D_{ji}} + \frac{1}{D_{j,K}} \right)^{-1}$$

In case of absence of the Knudsen diffusion, Wilke's law was used (Froment, et al., 2010), obtaining similar results to that obtained by the previous formula omitting the Knudsen term:

$$D_{jf} = \left(\frac{1}{1 - x_j} \sum_{\substack{i=1 \\ i \neq j}}^n \frac{x_i}{D_{ji}} \right)^{-1}$$

3.2.1.4. Global mass transfer coefficient

Previously, the coefficient $k_{g,j}$ has been introduced. It is necessary to make a deeper description of this term. As already mentioned, it takes into account the transport limitations that the chemical specie j has to overcome to reach the surface of a pellet. In particular, it quantifies the cubic meters of fluid which reaches each square meter

of the surface of a pellet in the unit of time. It is defined through correlations which involve the Sherwood number (which is analogous of the Nusselt one, but applied to the mass transport). In this thesis, it was used a relationship taken from (Bird, et al., 2002):

$$k_{g,j} = Sh_j \frac{D_{jf}}{D_p}$$

The Sherwood number was calculated using a correlation from (Bird, et al., 2002)

$$Sh_j = 1.09 \frac{(ReSc_j)^{1/3}}{\varepsilon_b}$$

where

$$Re = \frac{\rho_f u_f D_p}{\eta_f} \quad Sc_j = \frac{\eta_f}{\rho_f D_{jf}}$$

3.2.1.5. Experimental set up

Firstly, it was necessary to specify which kind of catalyst has been used for the simulation. The used catalytic bed was “constructed” inspiring to those of (Lim, et al., 2010) and (Graaf, et al., 1990): Lim et al. used cylindrical pellets of dimensions 5x3 mm (diameter x length); in this thesis, the catalyst was made of spherical pellets having the same volume of the those used in this reference. However, the kinetic expressions reported in Graaf et al., based on a commercial Cu-Zn-Al catalyst (Haldor Topsoe MK 101), was used (these kinetic formulations will be shown in a following paragraph). The bulk density and the void fraction of the bed were taken from (Lim, et al., 2010) and (Benenati & Brosilow, 1961) respectively, while the porosity of the pellet from (Green & Perry, 2007). The constructive features of the catalyst are listed in Table 3.2.

Table 3.2: Catalyst's constructive features

| Properties of the catalyst | |
|-----------------------------------|--------|
| Pellet diameter [m] | 0.0048 |
| Pellet porosity [-] | 0.3 |
| Pellet tortuosity [-] | 2.5 |
| Void fraction [-] | 0.39 |
| Bulk density [kg/m ³] | 952 |

The defined catalyst was inserted in a reactor with the features listed in Table 3.3. The tube's length was taken from (Arab, et al., 2014): the reference reports a possible variation of the length in the range [0.5;8] m; it was selected the highest value in order to avoid complications in the definition of the kinetics due to too low conversions. The tube's diameter of the pellet was chosen in such a way as to be equal to 15 times that of the pellet; this measure was due to the intention to avoid channelling phenomena (i.e. preferential pathway of the fluid inside the interstices of the porous matrix), which arise when the ratio between the tube's and the pellet's diameters is smaller than 10. The mass of catalyst was obtained as the result of the product between the volume of the reactor and the void fraction of the bed. Temperature and pressure were defined accordingly to (Atsonios, et al., 2016) and the thermodynamic evaluation previously performed.

Table 3.3: Reactor's features

| Properties of the reactor | |
|----------------------------------|--------|
| Tube's length [m] | 8 |
| Tube's diameter [m] | 0.0724 |
| Mass of catalyst [kg] | 31.364 |
| T [°C] | 250 |
| P [bar] | 65 |

The reactor was fed by a fluid with the feature in Table 3.4 The spatial velocity was taken from (Arab, et al., 2014): the reference reports a possible variation of the WHSV in the range [2;10] h⁻¹; it was selected the lowest value in order to avoid complications in the definition of the kinetics due to too low conversions. The mass flow rate reported in the table is the results of the product between the WHSV (obviously, converted in s⁻¹) and the mass of catalyst inside the reactor. The choice of using a stoichiometric feeding was in accord with (Arab, et al., 2014) and (Atsonios, et al., 2016), and confirmed by the evaluations previously done.

Table 3.4: Feeding's features

| Properties of the fluid | |
|---------------------------|----------------|
| Mass flow rate [kg/s] | 0.00483 |
| Feeding H2/CO2 (or H2/CO) | Stoichiometric |
| WHSV [h ⁻¹] | 2 |

3.2.1.6. Implemented kinetics

As previously mentioned, for the simulation of the reactions occurring inside the reactor, the kinetic expression elaborated by Graaf et al. were used. These formulations are reported below (Graaf, et al., 1990):

$$r_{CO_2hyd} = \frac{k'_{ps,CO_2hyd} K_{CO_2} (f_{CO_2} f_{H_2}^{3/2} - f_{CH_3OH} f_{H_2O} / (f_{H_2}^{3/2} K_{P,CO_2hyd}^0))}{(1 + K_{CO} f_{CO} + K_{CO_2} f_{CO_2}) (f_{H_2}^{1/2} + (K_{H_2O} / K_{H_2}^{1/2}) f_{H_2O})}$$

$$r_{RWGS} = \frac{k'_{ps,RWGS} K_{CO_2} (f_{CO_2} f_{H_2} - f_{H_2O} f_{CO} / K_{P,RWGS}^0)}{(1 + K_{CO} f_{CO} + K_{CO_2} f_{CO_2}) (f_{H_2}^{1/2} + (K_{H_2O} / K_{H_2}^{1/2}) f_{H_2O})}$$

$$r_{COhyd} = \frac{k'_{ps,COhyd} K_{CO} (f_{CO} f_{H_2}^{3/2} - f_{CH_3OH} / (f_{H_2}^{1/2} K_{P,COhyd}^0))}{(1 + K_{CO} f_{CO} + K_{CO_2} f_{CO_2}) (f_{H_2}^{1/2} + (K_{H_2O} / K_{H_2}^{1/2}) f_{H_2O})}$$

In this kinetic scheme, the reaction rates are expressed in the Langmuir – Hinshelwood form, with a numerator given by the product of a reaction rate constant and a driving force term, and a denominator given by the adsorption term. In these expressions, there are many quantities to be explained:

- *Reaction rate constants*: they were taken from (Graaf, et al., 1990) and have the following expressions:

$$k'_{ps,CO_2hyd} = (1.09 \pm 0.07) * 10^5 * \exp\left(\frac{-87500 \pm 300}{R_u T}\right) \quad [k'_{ps,CO_2hyd}] = \left[\frac{mol}{s \cdot kg \cdot bar}\right]$$

$$k'_{ps,RWGS} = (9.64 \pm 7.30) * 10^{11} * \exp\left(\frac{-152900 \pm 1800}{R_u T}\right) \quad [k'_{ps,RWGS}] = \left[\frac{mol}{s \cdot kg \cdot bar^{1/2}}\right]$$

$$k'_{ps,COhyd} = (4.89 \pm 0.29) * 10^7 * \exp\left(\frac{-113000 \pm 300}{R_u T}\right) \quad [k'_{ps,COhyd}] = \left[\frac{mol}{s \cdot kg \cdot bar}\right]$$

- *Adsorption equilibrium constants*: also these parameters were taken from (Graaf, et al., 1990):

$$K_{CO_2} = (7.05 \pm 1.39) * 10^{-7} * \exp\left(\frac{-61700 \pm 800}{R_u T}\right) \quad [K_{CO_2}] = \left[\frac{1}{bar}\right]$$

$$K_{CO} = (2.16 \pm 0.44) * 10^{-5} * \exp\left(\frac{-46800 \pm 800}{R_u T}\right) \quad [K_{CO}] = \left[\frac{1}{bar}\right]$$

$$K_{H_2O} / K_{H_2}^{1/2} = (6.37 \pm 2.88) * 10^{-9} * \exp\left(\frac{-84000 \pm 1400}{R_u T}\right) \quad [K_{H_2O} / K_{H_2}^{1/2}] = \left[\frac{1}{bar^{1/2}}\right]$$

- *Partial fugacities*: these quantities are comparable to partial pressure and allow for describing the behaviour of real gasses by the perfect gasses' equation of state (Cali & Gregorio, 1996). In this thesis, it was supposed to have ideal gasses; for this reason, they were substituted by partial pressure;
- *Thermodynamic equilibrium constant (based on partial pressures)*: these constants are generally determined by minimization of the Gibbs free energy, or by empirical correlations. (Graaf, et al., 1990) provide such a kind of expressions, but more updated and precise versions are given in (Graaf & Winkelman, 2016); for this reason, the correlations of the last reference were used, which give the equilibrium constants as a polynomial exponential function of temperature:

$$\ln K_{P,CO_{2}hyd}^0(T) = \frac{1}{R_u T} [a_1 + a_2 T + a_3 T^2 + a_4 T^3 + a_5 T^4 + a_6 T^5 + a_7 T \ln T]$$

$$a_1 = 7.44140 * 10^4 \quad a_2 = 1.89260 * 10^2 \quad a_3 = 3.2443 * 10^{-2} \quad a_4 = 7.0432 * 10^{-6}$$

$$a_5 = -5.6053 * 10^{-9} \quad a_6 = 1.0344 * 10^{-12} \quad a_7 = -6.4364 * 10^1$$

$$\ln K_{P,RWGS}^0(T) = \frac{1}{R_u T} [b_1 + b_2 T + b_3 T^2 + b_4 T^3 + b_5 T^4 + b_6 T^5 + b_7 T \ln T]$$

$$b_1 = -3.94121 * 10^4 \quad b_2 = -5.41516 * 10^1 \quad b_3 = -5.5642 * 10^{-2} \quad b_4 = 2.5760 * 10^{-5}$$

$$b_5 = -7.6594 * 10^{-9} \quad b_6 = 1.0161 * 10^{-12} \quad b_7 = 1.8429 * 10^1$$

$$K_{P,CO_{2}hyd}^0(T) = K_{P,CO_{2}hyd}^0(T) * K_{P,RWGS}^0(T)$$

3.2.1.7. Simulation and results

In order to obtain the data set mentioned earlier, it was decided to vary four parameters:

- *Temperature*: the range of variation [240;300] °C was selected, with a discretization step of 10 °C. This interval was bigger than that mentioned previously, [250;300] °C. The extension had the following purpose: taking the minimum value (given in (Arab, et al., 2014)) and the maximum one (above which the sintering of the catalyst starts), combined with a relatively small step, it was possible to carry out a careful analysis on the interval in which the optimal temperature (highlighted by (Gaikwad, et al., 2016)) falls;
- *Pressure*: the interval [20;95] bar was considered, which was subdivided with a step of 15 bar. This interval was bigger than that defined before, [50;100] bar. The extension was a consequence of the intention of analysing also pressures smaller than 50 bar, which characterize some applications;
- *Spatial velocity*: to be precise, WHSV was analysed. This quantity was varied, at 250 °C and 65 bar, in the interval [2;10] h⁻¹, accordingly to (Arab, et al., 2014);
- *Ratio between hydrogen and carbonaceous specie*: the composition of the feeding was varied, at 250 °C and 65 bar, in a range around the stoichiometric value, which is different per each reaction. These range were H₂/CO₂ ∈ [1;2;3;4;5] for CO₂ hydrogenation, H₂/CO₂ ∈ [1/3;1/2;1;2;3] for RWGS and H₂/CO ∈ [0.5;1;2;3;4] for CO hydrogenation.

Also the variation of the ratio between the tube's diameter and the pellet's one was evaluated, but not included in the data set: modifying the section of the reactor at fixed length, the volume of the reactor changed, and thus the mass of catalyst; since the incoming mass flow rate remained fixed, also the WHSV changed. In this way, it was not possible to consider only the effect of the variation of Dt/D_p .

The model was realized by the definition of a system of codes in MATLAB® environment. The first order ordinary differential equation corresponding to the axial direction was solved by the function *ode45* (which implements a Runge – Kutta method), starting from the inlet composition and using the solution of continuity equation in the pellets as a boundary condition in each section of the reactor. The second order ordinary differential equation expressing the mass conservation in the pellets was treated by the function *fsolve*, which is suitable for the solution of boundary value problem as the considered one.

During the realization of the model, it was expected to obtain decreasing trends of reactants' concentrations and increasing trends of products' ones. How can be noticed in Figure 3.7.a, Figure 3.8.a and Figure 3.9.a (which have been obtained for $WHSV=2 \text{ h}^{-1}$, $T=250 \text{ °C}$, $p=65 \text{ bar}$, stoichiometric compositions and $Dt/D_p=15$), the model respected this expectation. To verify the reliability of the constructed model in terms of order of magnitude of the results, the obtained reaction rates at section level (velocity of the reactions in each section, considering also the effect of diffusion limitations) were compared to those resulting by a one-dimensional axial homogeneous steady state study (the implementation of which is much easier than that of the heterogeneous one):

$$u_f \frac{dC_j}{dz} = \sum_i^{nr} v_{j,i} \rho_b r_{i,mc}$$

How can be deduced from Figure 3.7.b, Figure 3.8.b and Figure 3.9.b (which represent, in graphic terms, the anticipated comparison), the model gave a good representation of the phenomenon: the differences between the two trends were due to the influence of the porous catalytic matrix, which limited the transport of the substances.

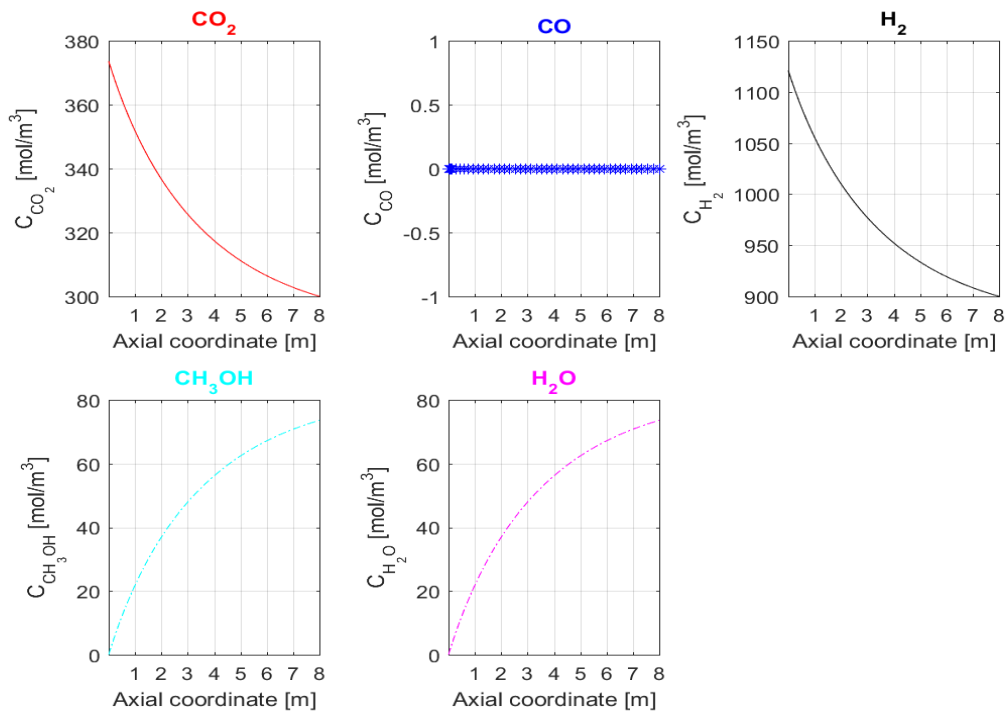


Figure 3.7.a: CO₂ hydrogenation: concentration profiles

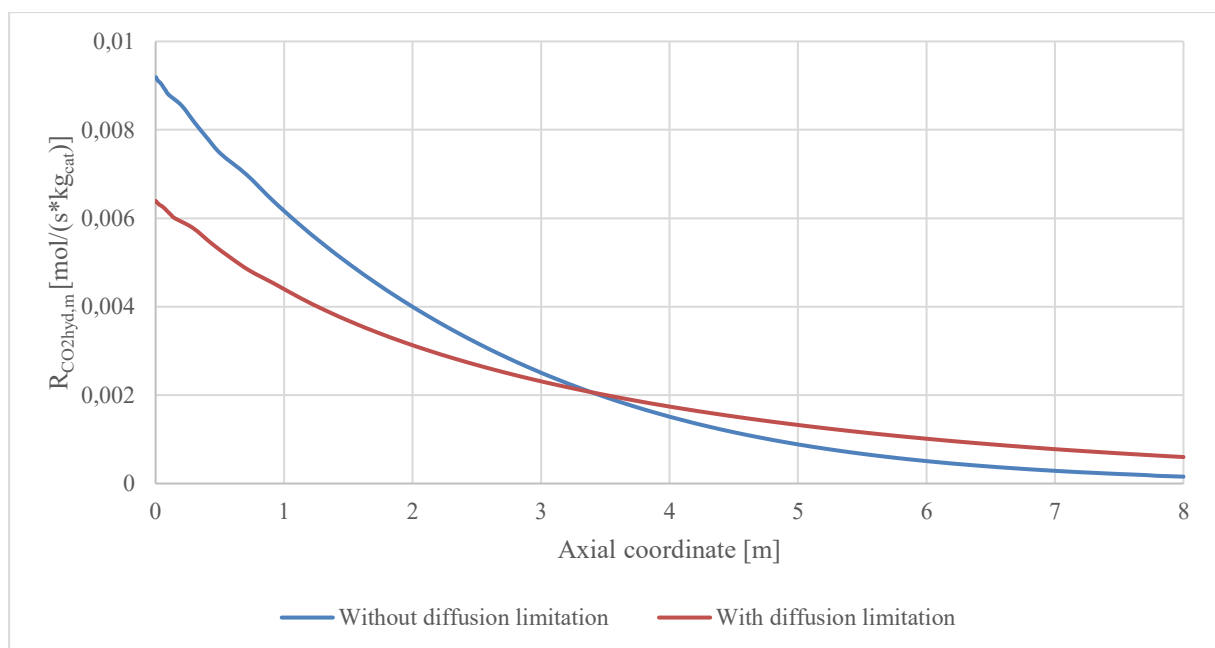


Figure 3.7.b: CO₂ hydrogenation reaction rates' comparison

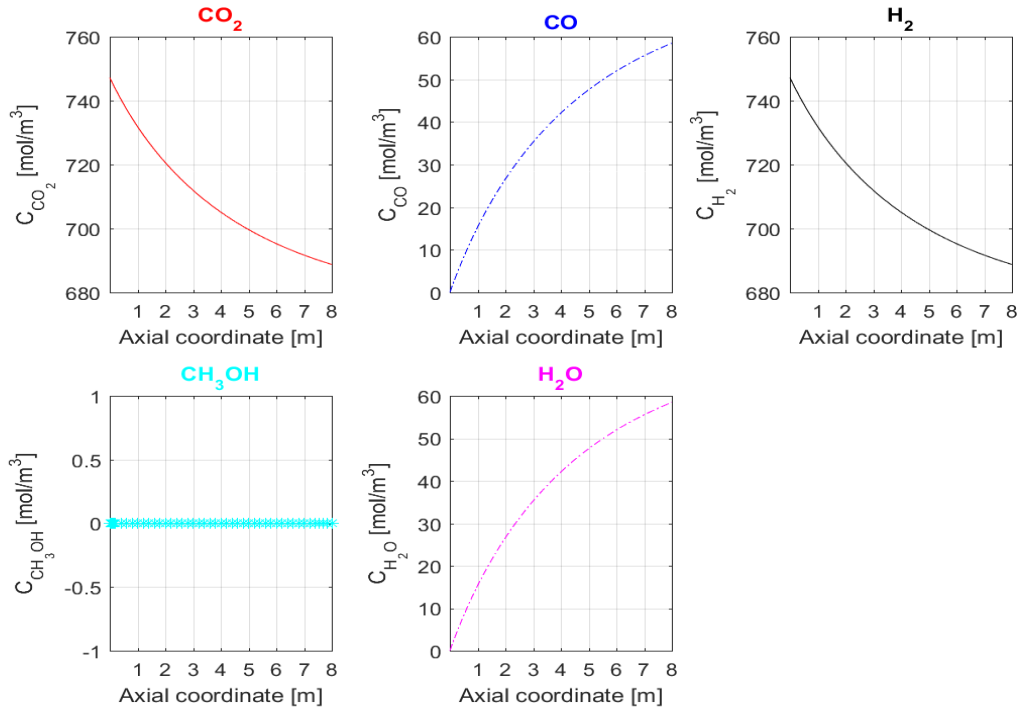


Figure 3.8.a: RWGS: concentration profiles

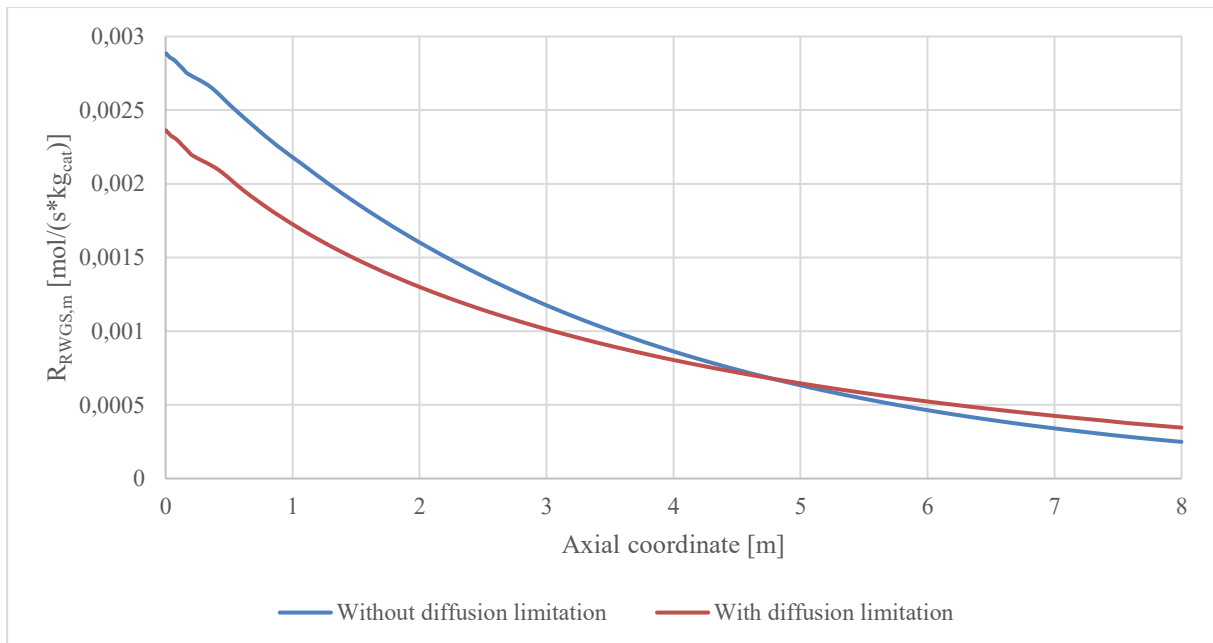


Figure 3.8.b: RWGS reaction rates' comparison

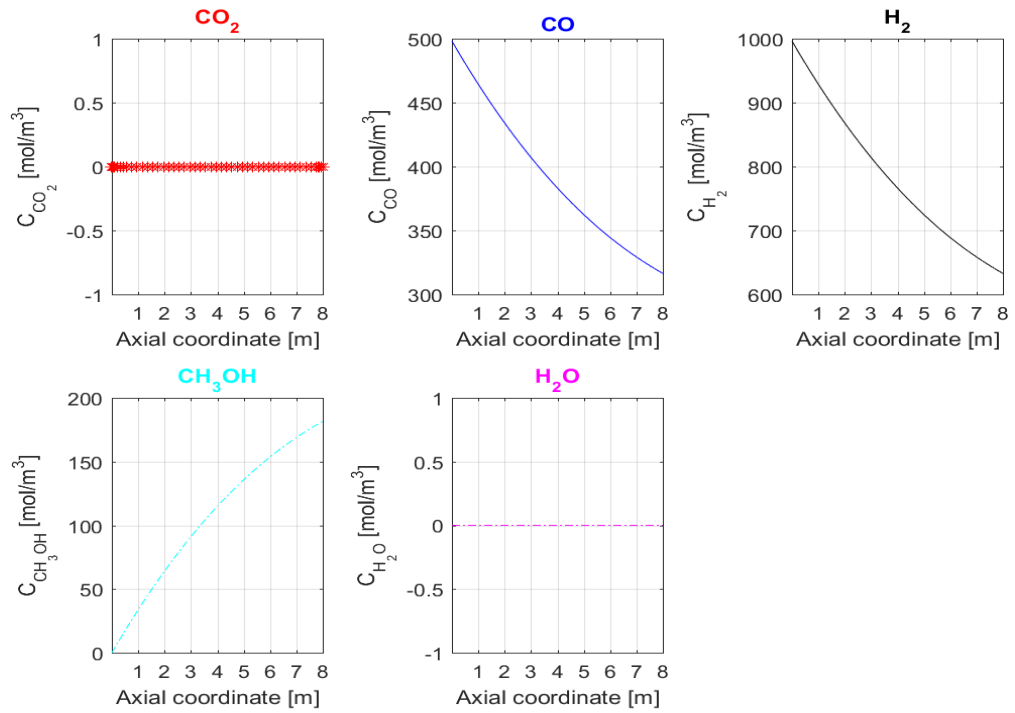


Figure 3.9.a: CO hydrogenation: concentration profiles

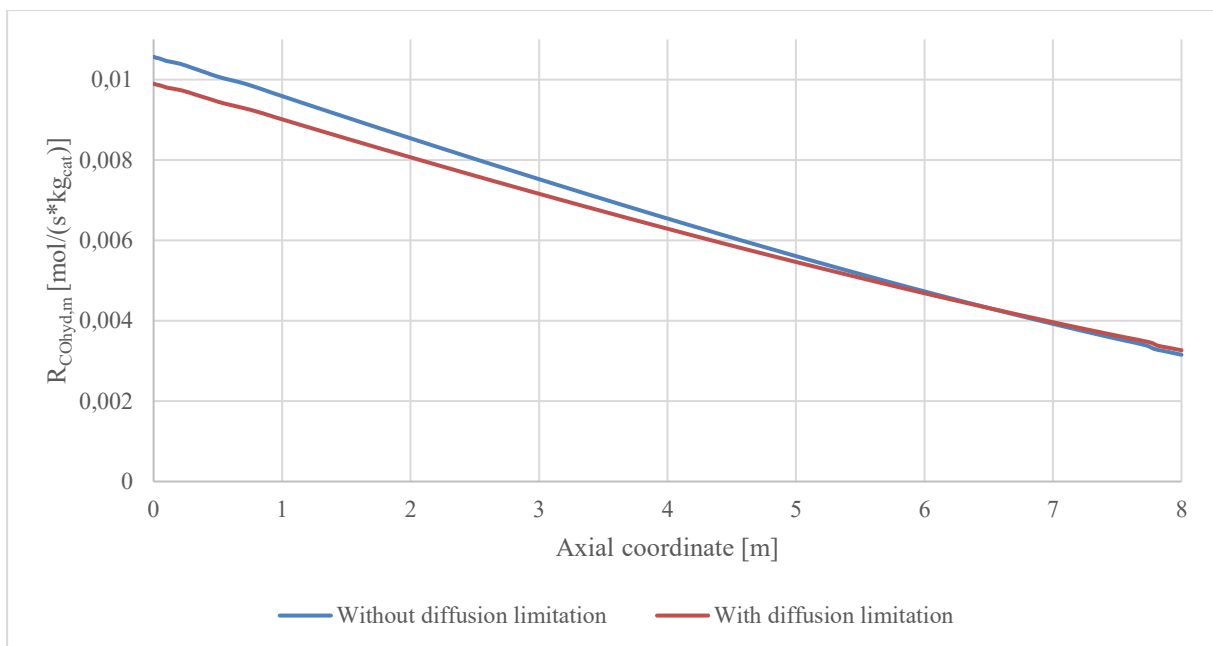


Figure 3.9.b: CO hydrogenation reaction rates' comparison

Basing on the results of the solution of the two differential equations, the conversion of the involved carbonaceous specie at the outlet of the reactor, in each experimental condition, was calculated for the three reactions (by the definition introduced at page 18).

3.2.2. Definition of a power-law kinetic scheme

The data set obtained by the described study was used as the reference in this part of the thesis, the aim of which was to determine the parameters allowing for the expression of the rates of reaction characterizing the process as power-laws:

$$r_{i,mc} = k_{\infty,i} e^{-\left(\frac{E_{a,i}}{R_u T}\right)} p_{R1}^{a_i} p_{R2}^{b_i} \left(1 - \frac{\prod_{j=1}^{n_s} p_j^{v_{j,i}}}{K_{P,i}^0}\right)$$

where R1 and R2 are the involved carbonaceous reactant (CO₂ or CO) and H₂ respectively. The kinetic parameters to be determined (for each reaction) were the following ones:

- *Pre-exponential factor* $k_{\infty,i}$ $\left[\frac{\text{mol}}{\text{s} \cdot \text{kg}_{\text{cat}} \cdot \text{bar}^{(a_i+b_i)}}\right]$;
- *Energy of activation* $E_{a,i}$ $\left[\frac{\text{J}}{\text{mol}}\right]$;
- *Exponent of the carbonaceous reactant* a_i [-];
- *Exponent of the hydrogen* b_i [-].

In order to find these quantities, the reactor was simulated, in the several experimental conditions considered in the previous section, by solving the PRF defining ordinary differential equation:

$$\frac{d\dot{n}_{j,i}}{dM_{\text{cat}}} - v_{j,i} r_{i,mc} = 0$$

where $\dot{n}_{j,i}$ is the molar flow rate of the specie j when considering only the reaction i. The meaning of the introduced equation has to be explained: in a PFR, the global reaction proceeds as the fluid flows along the tubes, crossing the catalyst, and ends when the outlet section has been reached; for this reason, it can be said that the chemical phenomenon advances as the encountered mass of catalytic material increases.

The obtained conversions (which will be called as “ode’s” ones) were used as comparison parameters with respect to those obtained in the previous study (which will be referred to as “model’s” ones) inside a fitting procedure implemented in MATLAB® environment. This proceeding was based on the minimization of the sum of the square errors of ode’s results with respect to model’s one. For each reaction, the procedure involved the following steps:

- a) *Definition of the parameters’ initial guess values*: the function used in the subsequent section of the code is greatly affected by the initial guess values, which have not to be too far from the final solutions (otherwise, the function could require long times to converge or even not arrive at convergence); thus, these had to be carefully selected. It was decided to define a preliminary function to determine a suitable guess vector. This function received, as input, the model data regarding the conditions of WHSV=2 h⁻¹, the corresponding mass flow rate, T=250 °C, p=65 bar, stoichiometric composition and conversion in these conditions. It worked solving the PFR defining ode with the sets of kinetic parameters defined below and finding which of them generated the smallest absolute error with respect to the model conversion:

- A vector of pre-exponential factors $k_{\infty,i} = \text{logspace}(0,5,6) \left[\frac{\text{mol}}{\text{s} \cdot \text{kg}_{\text{cat}} \cdot \text{bar}^{(a_i+b_i)}} \right]$, defined around a central value, whose order of magnitude was determined by attempts;
- An energy of activation $E_{a,i} = 10^5 \frac{\text{J}}{\text{mol}}$, whose value was coherent to those obtained in (Graaf, et al., 1990) and (Kobl, et al., 2016);
- a_i and b_i similar to the exponents of the corresponding partial pressures in the driving force term of the reaction rate expressions of (Graaf, et al., 1990):

$$a_{\text{CO}_2\text{hyd}} = 1 \quad b_{\text{CO}_2\text{hyd}} = 3/2$$

$$a_{\text{RWGS}} = 1 \quad b_{\text{RWGS}} = 1$$

$$a_{\text{COhyd}} = 1 \quad b_{\text{COhyd}} = 3/2$$

b) *Determination of the set of kinetic parameters minimizing the sum of the square errors:* in this step, all the experimental conditions treated during the data set generation were considered in a non-linear fitting procedure. The function *fminsearch* were used to reach the aim (Finlayson, 2012): starting from the guess vector previously defined, it varied several times the set of kinetic parameters; on the basis of each set, it calculated, in the different experimental conditions, the conversions at the exit of the reactor, the quadratic error with respect to the model's ones and the sum of these errors; it terminated its analysis when the considered kinetic parameters are satisfactory, since they generated a sum of the quadratic deviations smaller than a certain tolerance (the default value is 1e-4).

The sets of kinetic parameters obtained through the described procedure are reported in Table 3.5.

Table 3.5: kinetic parameters

| | CO₂ Hydrogenation | RWGS | CO Hydrogenation |
|---|-------------------------------------|-------------|-------------------------|
| $k_{\infty,i} \left[\frac{\text{mol}}{\text{kg}_{\text{cat}} \cdot \text{s} \cdot \text{bar}^{a_i+b_i}} \right]$ | 8.97E+05 | 7.05E+03 | 1.52E-03 |
| $E_{a,i} \left[\frac{\text{J}}{\text{mol}} \right]$ | 1.12E+05 | 7.99E+04 | 1.44E+04 |
| a_i [-] | 5.46E-01 | 1.49E-01 | -8.82E-02 |
| b_i [-] | 1.29E+00 | 6.86E-01 | 1.33E+00 |

The kinetic scheme was validated in a qualitative manner, by means of parity plots: considering the reactions one by one, the rates' expressions here defined were used to calculate, in the several experimental conditions, the conversion at the outlet of the reactor, obtained through the solution of the PFR defining ode; then, graphs which reported, in each condition, the ode's conversion (on the axis of the ordinates) as a function of the model's ones (on the axis of the abscissae) were drawn. A reliable kinetic scheme should give results not dissimilar from those obtained by the model; in graphical terms, the points corresponding to the various conditions should fall close to the bisector. Hence, the parity plots obtained in this study (Figure 3.10, Figure 3.11 and Figure 3.12) demonstrated that the defined power-law kinetic scheme was reliable.

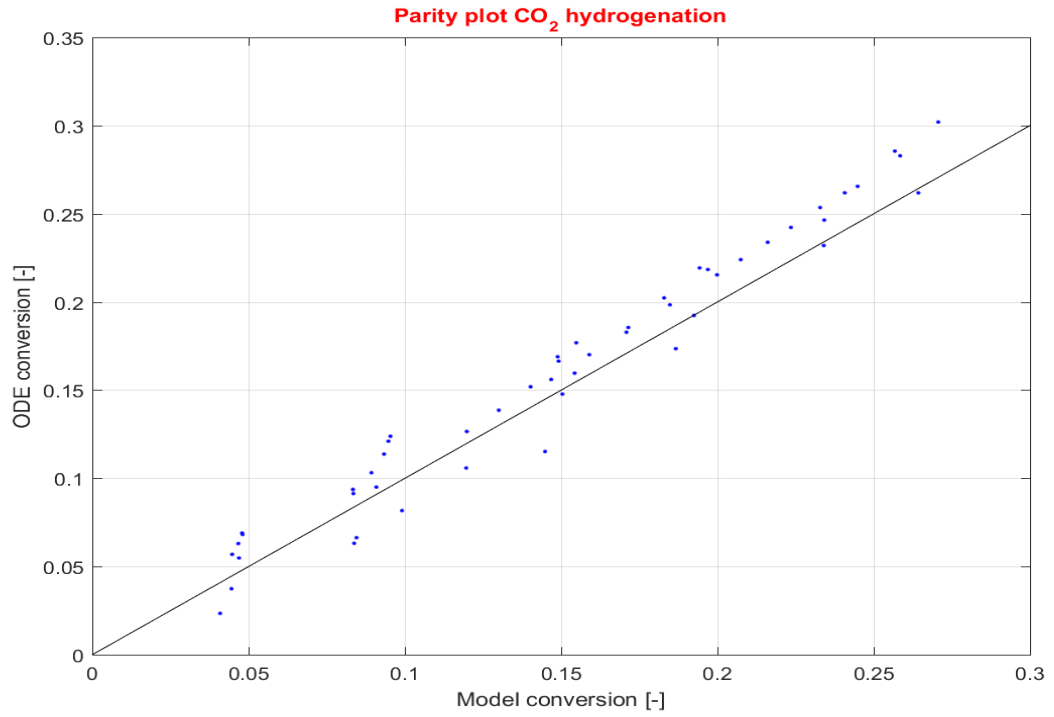


Figure 3.10: CO₂ hydrogenation: parity plot

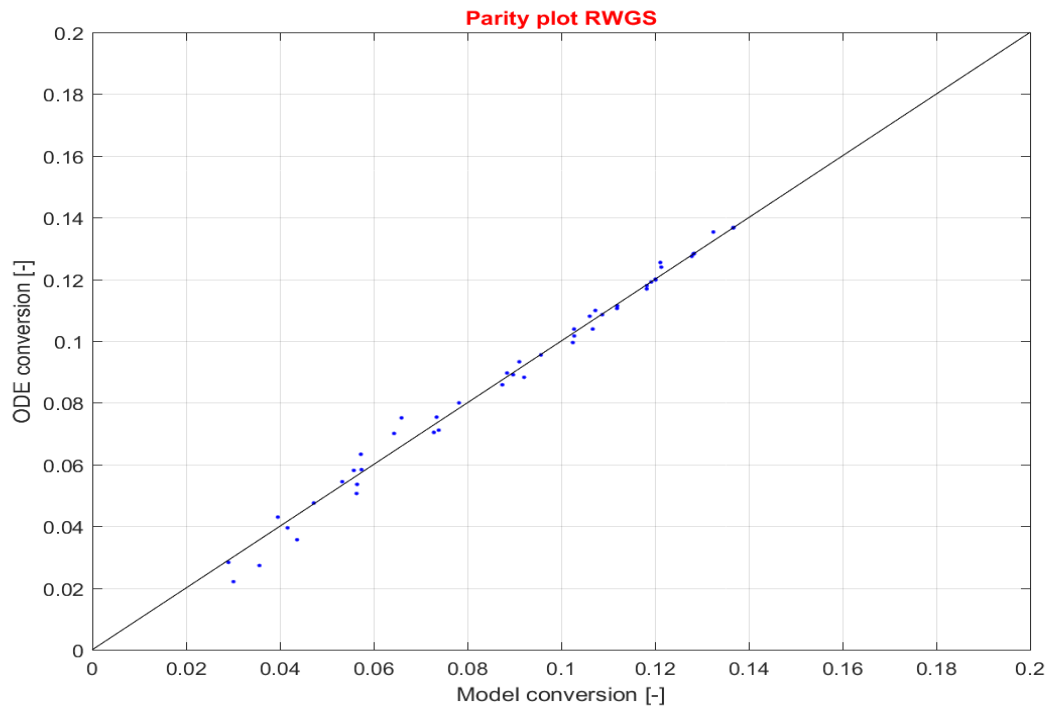


Figure 3.11: RWGS: parity plot

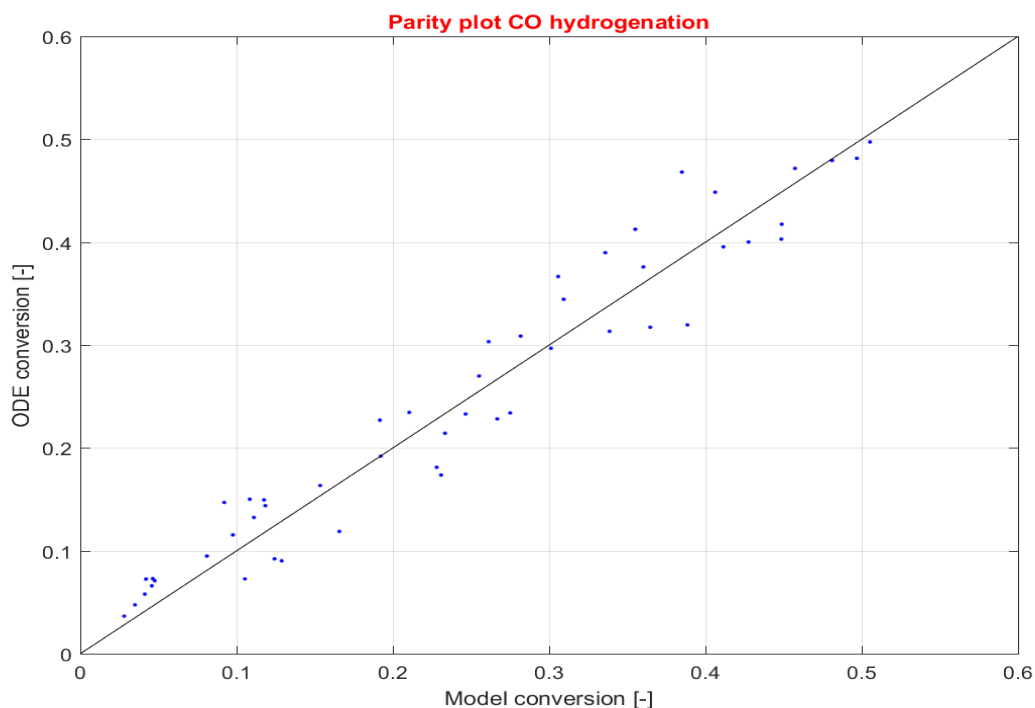


Figure 3.12: CO hydrogenation: parity plot

3.3. Plant's simulation and evaluation

3.3.1. Design of the plant

3.3.1.1. Initial decisions

Once obtained a reliable kinetic scheme, the following step was to realize the simulation of a plant which could produce methanol by CO₂ hydrogenation. As already mentioned, the aim of this system was to obtain the MeOH starting from the H₂O (to be converted in H₂ by electrolysis) and captured CO₂. The plant was simulated using Aspen Plus®. The first decision to make was how to size the plant; there were two alternatives:

1. To consider a certain CO₂ flow rate in input and size the electrolysis block (in terms of water input and installed power) and the reactor (concerning the number of tubes and their dimensions) according to the carbon dioxide to be processed;
2. To consider a certain installed power of the electrolysis block (with a consequent fixing of the water input) and select the CO₂ flow rate entering the plant and the reactor size (in terms of the number of tubes and their dimensions) according to the produced hydrogen.

In this thesis, it was chosen to follow the second option. Taking inspiration from the Audi's power to gas plant, located in Werlte (Germany), which converts carbon dioxide and hydrogen (obtained by electrolysis) into methane and has a size of 6 MW (Audi, n.d.), it was decided to simulate a plant with electrolysis installed power equal to about 10 MW. The second decision was the kind of electrolyser to be used. Considering that

alkaline ones are the most mature technology, it was chosen to use an Alkaline Hydrogen Generator HySTAT® - 100-10 from HYDROGENICS (HYDROGENICS, 2017): at nominal load, it produces 100 Nm³/h of hydrogen at a pressure of about 10 bar with a conversion efficiency of 5.4 kWh/ Nm³H₂; consequently, an electrolysis train made of 19 components has an installed power equal to 10.26 MW. Considering to run the electrolyzers at nominal load (at which they have the highest performances), it was possible to determine the inlet mass flow rate of water and carbon dioxide, which are resumed in Table 3.6; it was supposed to take water from the network (for this reason, at T= 15 °C and p=1.01325 bar) and to receive CO₂ at gasses' standard conditions (at T= 25 °C and p=1.01325 bar). Concerning the reactor, it was decided to simulate an isothermal multi-tubular PFR made of 3000 tubes (similar to the number considered in (Elkamel, et al., 2009)), which were characterized by a length of 4.3 m (an intermediate value with respect to the variation range given in (Arab, et al., 2014)) and a diameter equal to 23 times that of the pellets; the reaction was performed at T=250 °C with p_{in}=65 bar, as suggested in (Atsonios, et al., 2016) (all this information is resumed in Table 3.7). The pressure drop inside the reactor, due to the presence of the catalyst, was calculated by Ergun's equation (Arab, et al., 2014):

$$-\frac{dp}{dz} = 150 \frac{(1 - \varepsilon_b)^2 \mu_f u_f}{\varepsilon_b D_p^2} + 1.75 \frac{1 - \varepsilon_b \mu_f u_f^2}{\varepsilon_b^3 D_p}$$

The last thing to do was to choose how to simulate the pressure changers that surely the system would have required. It was decided to consider isentropic components and to fix an isentropic efficiency equal to 0.75 for compressors and 0.7 for pumps (Atsonios, et al., 2016).

Table 3.6: Resources to be processed

| | Inlet H₂O | Inlet CO₂ |
|-----------------------|-----------------------------|-----------------------------|
| Mass flow rate [kg/h] | 1525.83 | 1243.265 |
| p [bar] | 1.01325 | 1.01325 |
| T [°C] | 15 | 25 |

Table 3.7: Reactor's constructive features and set up

| Properties of the reactor | |
|----------------------------------|---------|
| Tube's length [m] | 4.3 |
| Tube's diameter [m] | 0.11103 |
| Number of tubes | 3000 |
| T [°C] | 250 |
| P in [bar] | 65 |

3.3.1.2. Simulation on Aspen Plus®

Inspiring to (Atsonios, et al., 2016) and (Van-Dal & Bouallou, 2013), it was designed a plant, whose scope was to produce methanol, starting from carbon dioxide and hydrogen obtained as previously specified, with a purity of the 99.9%. The resulting system is very articulated, but can be essentially divided into two main parts:

- The *preparation section*, which has the task of bringing the reactants to the process conditions;
- The *processing section*, which is responsible for making the reaction take place, separating the unused reactants from the products, recirculating the firsts and subdividing the seconds into methanol, on one side, and remaining substances, on the other side.

For this reason, the two sections will be explained separately.

Preparation section

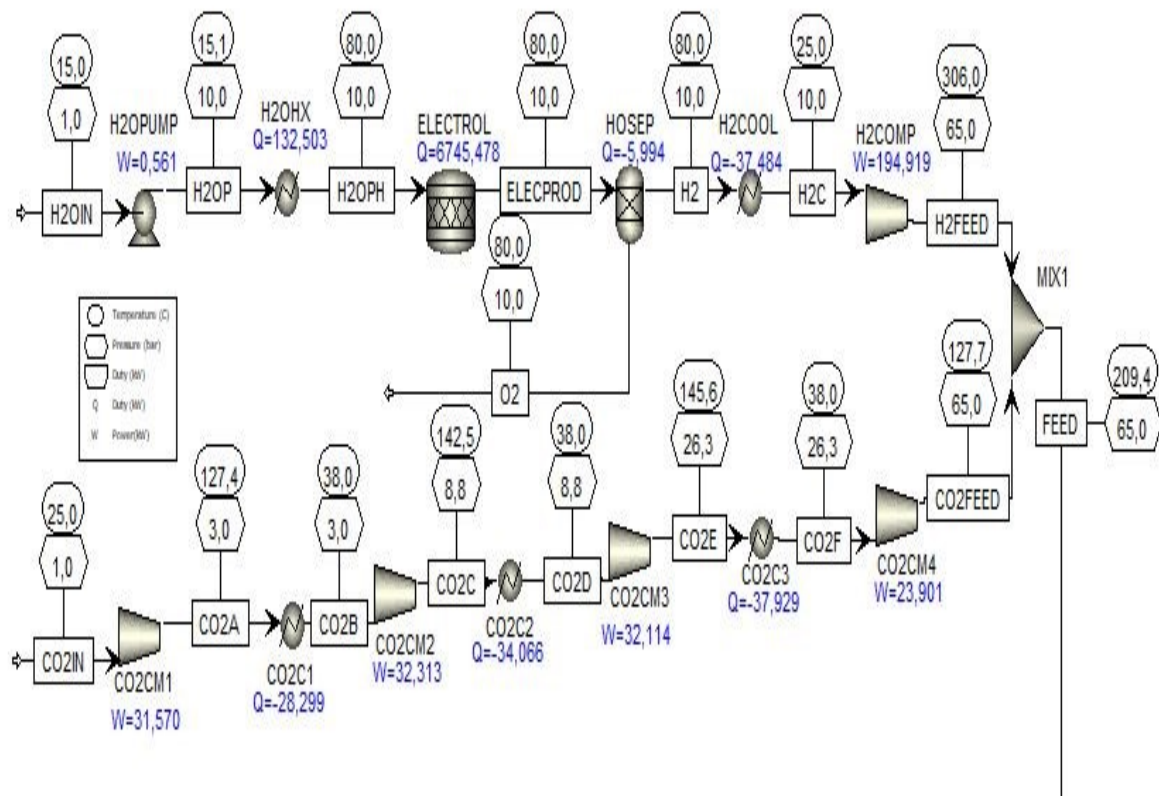


Figure 3.13: preparation section's scheme

In Figure 3.13, the preparation process is schematised. It is better to analyse the hydrogen line and the carbon dioxide one separately:

Figure 3.14 represents the core of the plant. The feeding flow (which is at a lower temperature than that of reaction) is mixed with the recirculated reactants (whose temperature is very low if compared with the reaction one); consequently, before entering the reactor, the resulting flow has to be preheated. A first preheating, up to a temperature of 150,7 °C (Atsonios, et al., 2016), is accomplished thanks to a heat exchange with the flow coming out of the reactor. Thereafter, a second heater brings the fluid to the process temperature. The flow exiting from the reactor, in addition to the aforementioned initial exchanger, undergoes two successive precooling, the first of which supplies heat for the preheating of the flow at the inlet of the distillation column. This series of coolers is used to bring the fluid leaving the reactor to the operating conditions of the first flash separator (T=30 °C, p=65 bar) (Atsonios, et al., 2016). In this component, there is the separation of methanol and water (liquids at the aforementioned conditions) from a considerable part of the reactants (CO₂, CO, H₂, gaseous). Both flows exiting from the component contain traces of the compounds destined to the other flow; in particular, the liquid phase contains a considerable fraction of carbon dioxide. Therefore, a second flash separator is required. The fluid reaches it crossing two rolling valves, which reduce the pressure up to 18.8 bar and the temperature up to 24.5 °C (T was taken from (Atsonios, et al., 2016)). Subsequently, the separator causes a flash separation, bringing the pressure to 2.2 bar; in this way, most of the reactants previously mixed with the products pass into the gaseous state and are recirculated. However, the problem of traces of undesired compounds in each flow leaving the separator still exists. The gaseous flows emerging from the flash separators are mixed (obviously, the one leaving the component at lower pressure is previously compressed up to the reactor pressure); afterwards, a small fraction (<1%) of the flow is removed (to avoid the accumulation of the products in the reactor, which would damage the position of the equilibrium of the reaction) (Atsonios, et al., 2016). The remaining part is compressed up to reactor pressure (compensating for the slight expansion due to the removal) and mixed with fresh reactants. The liquid fraction leaving the second separator consists essentially of methanol and water. To separate the MeOH from the rest, after the previously mentioned preheating (up to 85 °C, (Atsonios, et al., 2016)), the distillation column is used. It has been modelled considering a number of stages equal to 60 (Atsonios, et al., 2016), with pressure equal to the atmospheric one at the condenser and to 1.1 bar at the reboiler, in order to produce methanol with a degree of purity of 99.9% (similar to the 99.3% of (Atsonios, et al., 2016)). It is worth noting the thermal levels of the two produced flows (methanol has a very low temperature, water a relatively high one), which lead themselves to further thermal integrations.

3.3.2. Plant efficiency assessment

Once the system was simulated, it was necessary to evaluate its first principle efficiency, defined in the following way:

$$\varepsilon = \frac{\text{Chemical power of produced MeOH}}{\text{Electrical power used for the production}} * 100 = \frac{\dot{m}_{MeOH} LHV_{MeOH}}{W_{el,global}} * 100 \quad [\varepsilon] = [\%]$$

The numerator was known: the mass flow rate of produced methanol was obtained from Aspen Plus[®], while the lower heating value was taken from literature. On the contrary, the denominator was more complex to be defined: it was supposed to satisfy the heat requirement of the system by an electric heater (having unitary

global efficiency of generation and exchange). Thus, the definition of the denominator passed through a procedure of determination of the minimum required heat. For this reason, the two terms are treated separately.

3.3.2.1. Chemical power of produced methanol

As mentioned before, in Table 3.8 there are the mass and molar flow rates of produced methanol, obtained through the simulation in Aspen Plus®, and its lower heating value. Starting from them, the electrical power converted in the chemical one by the generation of methanol was obtained by a simple multiplication.

Table 3.8: chemical power evaluation

| MeOH _{out} [kg/s] | MeOH _{out} [kmol/s] | LHV _{MeOH} [kJ/kg] | <u>MeOH chemical power [kW]</u> |
|----------------------------|------------------------------|-----------------------------|---------------------------------|
| 0,219 | 0,0068 | 19920 | 4361,331 |

3.3.2.2. Electrical power used to produce methanol

Determination of the maximum and minimum thermal requirements and of the pinch point

As told, an evaluation of the minimum required heat is needed. In this study, a $\Delta T_{min} = 10\text{ }^{\circ}\text{C}$ was considered. The fluxes to be combined to minimize the external heat requirement were those in Table 3.9. Initially, the fluids were called with the names of the crossed components. In general, starting from the inlet and outlet temperatures and mass enthalpies and the mass flow rate, the specific heat c and the product Gc were determined. Then, by the formula $\dot{Q}_{calc} = (Gc)_i(T_{in} - T_{out})$, the resulting heat powers were calculated (with this definition, the convention if positive heat when given to the fluid is satisfied). The reactor, the second flash separator and the heat exchangers of the distillation column were more complicated to be considered: it was known the exchanged thermal powers and the mass flow rates, but not the variation of temperature. In order to deal with the heat of the reactor, it was represented as a hot fluid to be cooled down of a $\Delta T^* = 1\text{ }^{\circ}\text{C}$ (in other words, it was substituted with a changing phase refrigerant). The same approach was applied to the heat exchangers of the distillation column, considering $\Delta T^* = 1\text{ }^{\circ}\text{C}$ for the condenser (COND) and $\Delta T^* = -1\text{ }^{\circ}\text{C}$ for the reboiler (REB). A similar concept was used for the evaluation of the second flash separator: it was approximated with a unique fluid, having the mass flow rate of the fluid entering the component, which had to be heated up of a $\Delta T^* = 1\text{ }^{\circ}\text{C}$. Once supposed the variation of temperature, all these fluids could be treated as the other. As it can be noticed, the difference between the effective thermal powers and the calculated ones were acceptable; for this reason, the \dot{Q}_{calc} were successively considered. Table 3.10 reports the fluids, subdivided in hot ones and cold ones, with the respective fictitious temperatures. Summing up the heat requirements of cold fluids and the heat releases of the hot ones, the maximum heating and cooling needs were obtained (Table 3.11).

Table 3.9: fluids to be heated or cooled

| Fluid's name | Type | T _{in} [°C] | T _{out} [°C] | h _{in} [J/kg] | h _{out} [J/kg] | c [kJ/(kgK)] | G [kg/s] | Gc [kW/K] | Q [kW] | Q _{calc} [kW] |
|--------------|------|----------------------|-----------------------|------------------------|-------------------------|--------------|----------|-----------|-----------|------------------------|
| H2OHX | cold | 15,1 | 80,0 | -16081000 | -15769000 | 4,806 | 0,424 | 2,037 | 132,503 | -132,239 |
| H2COOL | hot | 80,0 | 25,0 | 794643 | 4299,702 | 14,370 | 0,047 | 0,682 | -37,484 | 37,484 |
| CO2C1 | hot | 127,4 | 38,0 | -8850900 | -8932900 | 0,918 | 0,345 | 0,317 | -28,299 | 28,319 |
| CO2C2 | hot | 142,5 | 38,0 | -8839300 | -8937900 | 0,944 | 0,345 | 0,326 | -34,066 | 34,052 |
| CO2C3 | hot | 145,6 | 38,0 | -8845000 | -8954800 | 1,020 | 0,345 | 0,352 | -37,929 | 37,920 |
| F1C1C | cold | 51,7 | 150,7 | -6463600 | -6173500 | 2,930 | 3,169 | 9,284 | 919,152 | -919,331 |
| RPH | cold | 150,7 | 250,0 | -6173500 | -5847700 | 3,281 | 3,169 | 10,397 | 1032,630 | -1032,465 |
| PFR | hot | 251,0 | 250,0 | -5847700 | -5982300 | 134,600 | 3,169 | 426,549 | -426,725 | 426,549 |
| F1C1H | hot | 250,0 | 161,1 | -5982300 | -6272400 | 3,265 | 3,169 | 10,347 | -919,152 | 919,331 |
| F1C2H | hot | 161,1 | 148,5 | -6272400 | -6312100 | 3,145 | 3,169 | 9,967 | -124,939 | 125,810 |
| F1C3 | hot | 148,5 | 30,0 | -6312100 | -6884200 | 4,827 | 3,169 | 15,296 | -1813,006 | 1812,994 |
| FLASH2 | cold | 23,5 | 24,5 | - | - | 125,105 | 0,620 | 77,539 | 77,539 | -77,539 |
| F1C2C | cold | 24,5 | 85,0 | -10575000 | -10233000 | 5,653 | 0,365 | 2,062 | 124,939 | -124,740 |
| COND | hot | -17,8 | -18,8 | - | - | 1774,281 | 0,240 | 425,840 | -425,840 | 425,840 |
| REB | cold | 103,5 | 104,5 | - | - | 2507,206 | 0,125 | 312,725 | 312,725 | -312,725 |

Table 3.10: reordered fluids with fictitious temperatures

| Fluid's name | Fluid's number | Type | T _{in} [°C] | T _{out} [°C] | T _{in} * [°C] | T _{out} * [°C] | Gc [kW/K] | Q _{calc} [kW] |
|--------------|----------------|------|----------------------|-----------------------|------------------------|-------------------------|-----------|------------------------|
| H2COOL | 1 | hot | 80,0 | 25,0 | 75,0 | 20,0 | 0,682 | 37,484 |
| CO2C1 | 2 | hot | 127,4 | 38,0 | 122,4 | 33,0 | 0,317 | 28,319 |
| CO2C2 | 3 | hot | 142,5 | 38,0 | 137,5 | 33,0 | 0,326 | 34,052 |
| CO2C3 | 4 | hot | 145,6 | 38,0 | 140,6 | 33,0 | 0,352 | 37,920 |
| PFR | 5 | hot | 251,0 | 250,0 | 246,0 | 245,0 | 426,549 | 426,549 |
| F1C1H | 6 | hot | 250,0 | 161,1 | 245,0 | 156,1 | 10,347 | 919,331 |
| F1C2H | 7 | hot | 161,1 | 148,5 | 156,1 | 143,5 | 9,967 | 125,810 |
| F1C3 | 8 | hot | 148,5 | 30,0 | 143,5 | 25,0 | 15,296 | 1812,994 |
| COND | 9 | hot | -17,8 | -18,8 | -22,8 | -23,8 | 425,840 | 425,840 |
| H2OHX | 10 | cold | 15,1 | 80,0 | 20,1 | 85,0 | 2,037 | -132,239 |
| F1C1C | 11 | cold | 51,7 | 150,7 | 56,7 | 155,7 | 9,284 | -919,331 |
| RPH | 12 | cold | 150,7 | 250,0 | 155,7 | 255,0 | 10,397 | -1032,465 |
| FLASH2 | 13 | cold | 23,5 | 24,5 | 28,5 | 29,5 | 77,539 | -77,539 |
| F1C2C | 14 | cold | 24,5 | 85,0 | 29,5 | 90,0 | 2,062 | -124,740 |
| REB | 15 | cold | 103,5 | 104,5 | 108,5 | 109,5 | 312,725 | -312,725 |

Table 3.11: maximum heating and cooling requirements

| $Q_{\max, \text{heating}}$ [kW] | $Q_{\max, \text{cooling}}$ [kW] |
|---------------------------------|---------------------------------|
| 3848,298 | 2599,039 |

The following step to do was the determination of the position of the pinch point and of the minimum heating and cooling requirements. This was done by the procedure shown in Table 3.12. The results are summarized in Table 3.13 and Table 3.14. As it can be deduced from Table 3.14, the pinch point is located at the inlet of the reactor. From Table 3.11 and Table 3.13, the realization of a net of heat exchanger would lead to a radical diminution of the thermal requirements. Moreover, it has to be considered that the fluid requiring the biggest cooling is that of the cooler F1C3, which needs a low temperature refrigerant to be cooled. Part of the heat could be removed, for example, by the methanol at the outlet of the plant, which would remain liquid during the entire heat exchange. This thermal integration would slightly decrease the cooling need.

Table 3.12: procedure of determination of the minimum heating and cooling requirements and of the pinch point

| Range number | T_i^* [°C] | T_{i+1}^* [°C] | Involved fluids | $\sum Gc_{\text{hots}} - \sum Gc_{\text{colds}}$ | Q_h [kW] | Q_i ($Q_1=0$) [kW] | Q_i ($Q_1=93,577$) [kW] |
|--------------|--------------|------------------|-----------------|--|------------|------------------------|-----------------------------|
| | | | | | | 0,000 | 93,577 |
| 1 | 255,0 | 246,0 | 12 | -10,397 | -93,577 | | |
| | | | | | | -93,577 | 0,000 |
| 2 | 246,0 | 245,0 | 5 12 | 416,152 | 416,152 | | |
| | | | | | | 322,575 | 416,152 |
| 3 | 245,0 | 156,1 | 6 12 | -0,051 | -4,499 | | |
| | | | | | | 318,076 | 411,652 |
| 4 | 156,1 | 155,7 | 7 12 | -0,430 | -0,193 | | |
| | | | | | | 317,883 | 411,460 |
| 5 | 155,7 | 143,5 | 7 11 | 0,683 | 8,316 | | |
| | | | | | | 326,199 | 419,776 |
| 6 | 143,5 | 140,6 | 8 11 | 6,012 | 17,496 | | |
| | | | | | | 343,695 | 437,272 |
| 7 | 140,6 | 137,5 | 4 8 11 | 6,364 | 19,935 | | |
| | | | | | | 363,630 | 457,207 |
| 8 | 137,5 | 122,4 | 3 4 8 11 | 6,690 | 101,155 | | |
| | | | | | | 464,786 | 558,362 |
| 9 | 122,4 | 109,5 | 2 3 4 8 11 | 7,007 | 90,173 | | |
| | | | | | | 554,959 | 648,536 |
| 10 | 109,5 | 108,5 | 2 3 4 8 11 15 | -305,718 | -305,718 | | |
| | | | | | | 249,241 | 342,817 |
| 11 | 108,5 | 90,0 | 2 3 4 8 11 | 7,007 | 129,592 | | |
| | | | | | | 378,833 | 472,410 |
| 12 | 90,0 | 85,0 | 2 3 4 8 11 14 | 4,945 | 24,726 | | |

| | | | | | | | |
|----|-------|-------|--------------------|---------|---------|----------|----------|
| | | | | | | 403,559 | 497,136 |
| 13 | 85,0 | 75,0 | 2 3 4 8 10 11 14 | 2,908 | 29,084 | | |
| | | | | | | 432,643 | 526,220 |
| 14 | 75,0 | 56,7 | 1 2 3 4 8 10 11 14 | 3,590 | 65,769 | | |
| | | | | | | 498,412 | 591,989 |
| 15 | 56,7 | 33,0 | 1 2 3 4 8 10 14 | 12,874 | 304,856 | | |
| | | | | | | 803,267 | 896,844 |
| 16 | 33,0 | 29,5 | 1 8 10 14 | 11,879 | 41,577 | | |
| | | | | | | 844,844 | 938,421 |
| 17 | 29,5 | 28,5 | 1 8 10 13 | -63,598 | -63,598 | | |
| | | | | | | 781,246 | 874,823 |
| 18 | 28,5 | 25,0 | 1 8 10 | 13,941 | 48,793 | | |
| | | | | | | 830,039 | 923,616 |
| 19 | 25,0 | 20,1 | 1 10 | -1,355 | -6,672 | | |
| | | | | | | 823,367 | 916,943 |
| 20 | 20,1 | 20,0 | 1 | 0,682 | 0,052 | | |
| | | | | | | 823,419 | 916,996 |
| 21 | 20,0 | -22,8 | - | 0,000 | 0,000 | | |
| | | | | | | 823,419 | 916,996 |
| 22 | -22,8 | -23,8 | 9 | 425,840 | 425,840 | | |
| | | | | | | 1249,259 | 1342,836 |

Table 3.13: minimum heating and cooling requirements

| $Q_{\min, \text{heating}} [\text{kW}]$ | $Q_{\min, \text{cooling}} [\text{kW}]$ |
|--|--|
| 93,577 | 1342,836 |

Table 3.14: pinch point

| $T_{pp}^* [^{\circ}\text{C}]$ | $T_{pp, \text{hots}} [^{\circ}\text{C}]$ | $T_{pp, \text{colds}} [^{\circ}\text{C}]$ |
|-------------------------------|--|---|
| 246 | 251 | 241 |

Calculation of the global electric power

Once obtained the minimum heating requirement (which had to be satisfied by an electrical heater), all the needed quantities for the calculation of the global electric power required were available. The single components' requirements and their summation are shown in Table 3.15: as it can be noticed, the electric power employed for heating purpose, like those required for the compression of the hydrogen and of the

gaseous flow recirculated from the second flash separator, is only marginally relevant; all the electric needs are negligible with respect to that of the electrolysis.

Table 3.15: electric powers

| Component | Power [kW] |
|---------------------------|----------------|
| H2OPUMP | 0,56 |
| ELECTROLYSIS | 10260,00 |
| H2COMP | 194,92 |
| CO2CM1 | 31,57 |
| CO2CM2 | 32,31 |
| CO2CM3 | 32,11 |
| CO2CM4 | 23,90 |
| RECC | 0,000596776005 |
| F2GC | 93,85 |
| Q _{min, heating} | 93,58 |
| W _{el, global} | 10762,81 |

3.3.2.3. Efficiency calculation and considerations

At this point, all the needed data to calculate the first principle efficiency were available. The result was an efficiency:

$$\varepsilon = 40.52\%$$

This efficiency was obtained with a *plant MeOH yield with respect to inlet CO₂*

$$Y = \frac{\text{Produced kmol of MeOH}}{\text{Captured kmol of CO}_2} * 100 = \frac{0.0068}{0.0078} * 100 = 87.08\%$$

The calculation of the efficiency in the case of total conversion of the captured CO₂ could have been useful to evaluate the goodness of the obtained data. For this reason, we supposed to have produced about 0.0078 kmol of methanol, i.e.:

$$Y^* = \frac{\text{Produced kmol of MeOH} = \text{Captured kmol of CO}_2}{\text{Captured kmol of CO}_2} * 100 = 100\%$$

To calculate the efficiency in this hypothetical case, we would have to recalculate both the numerator and the denominator. The former was easy to recalculate, but for the latter another simulation of the process and evaluation of the minimum heating need would have been necessary, since all the powers of the processing section would have changed (those of the flash separators and of the recirculating compressor would have been null, while those of the heat exchangers and of the column would have been different). However, a good estimate of the efficiency could have been obtained by placing the electrical power obtained in our “real” case at the denominator: as it has been demonstrated, it is mainly given by the electrolysis’ power, while the other

components have only marginal effects. Hence, only the nominator had to be recalculated. The result is shown in Table 3.16.

Table 3.16: chemical power evaluation in the hypothetical case

| MeOH out [kg/s] | MeOH out [kmol/s] | LHV MeOH [kJ/kg] | <u>MeOH chemical power</u> <u>[kW]</u> |
|-----------------|-------------------|------------------|---|
| 0,251 | 0,0078 | 19920 | 5002,087 |

Hence, the efficiency in this hypothetical case, which represents the maximum efficiency that can be reached with the selected flow rates of reactants, is:

$$\varepsilon^* = \frac{\text{Produced kmol of MeOH} = \text{Captured kmol of CO}_2}{\dot{W}_{el,global}} * 100 = \frac{5002,087}{10762.81} * 100 = 46.48\%$$

So, it can be concluded that the performances of the “real” plant are satisfactory.

4. Conclusions

The aim of this thesis was to study the phenomenon of CO₂ hydrogenation and to apply it in the design of a plant employing captured carbon dioxide and hydrogen obtained through water electrolysis to produce methanol. After an introduction focusing on the context that makes it necessary to develop new methods of treatment of carbon dioxide emitted into the atmosphere and on the advantages that the considered technology allows to obtain, an overview of the hydrogenation process and of the relevant literature regarding this topic has been presented. Afterwards, the results of the performed simulations have been exposed. The first step has been the analysis of the thermodynamic study, which has suggested to consider a high reaction pressure, a low reaction temperature and a stoichiometric composition (or a little in excess of hydrogen) of the feeding. However, this study took into account only thermodynamic effects and not also kinetic ones; for this reason, in the subsequent kinetic study was taken (from the literature) a temperature a little higher than that suggested by our thermodynamic evaluation as the reference value, while reference pressure and composition were coherent to our results. In order to obtain a reactor kinetic scheme consisting of power-law expressions, a data set was constructed by simulating the process (singularly considering each involved reaction) under several temperatures, pressures, feeding compositions and spatial velocities with a one-dimensional axial heterogeneous steady-state model. This data set was used as the reference for the definition of a non-linear fitting procedure, which solved, in the several conditions, the PFR defining ordinary differential equation and compared the obtained conversions with those of the previous model; the results were three sets of kinetic parameters (one for each reaction). The kinetic scheme was used to simulate a plant, sized on the installed power of the electrolysis train, in which a multi-tubular PFR produced methanol from captured CO₂ and obtained H₂. Through a procedure of determination of the minimum heating need (which was supposed to be electrically satisfied), the required electric power was assessed, concluding that electrolysis was the process

with the most significant demand for electricity. The following step was the calculation of the efficiency, which was established to be satisfactory. It could be interesting, to further study this kind of process:

- To perform a comparison among one-dimensional and two-dimensional, homogeneous and heterogeneous, models in terms of committed error and computational cost;
- To use, instead of *fminsearch*, which is part of the MATLAB® Optimization Tool, a function of the Statistical Tool, like *nlinfit*, in order to obtain a quantitative evaluation of the reliability of the obtained kinetic scheme;
- To do a sensitivity analysis to find the optimal pressures for the flash separators and for the distillation column's heat exchanger;
- To design a net of heat exchanger realizing the minimum thermal requirements which have been calculated;
- To consider the effect of a reintegration of the water extracted at the distillation column;
- To evaluate, in relation to the storage conditions of methanol and to the desired use of produced water, to realize heat exchanger for the thermal integration of these two fluids;
- To evaluate which could be the final use of extracted O₂;
- To perform also an economic analysis of the plant, arriving at a thermo-economic evaluation which would allow optimizing the plant on both the aspects.

Appendix: electrolyser's thermal balance

This balance consists of two opposite contributions:

1. *Chemical contribution*: the water electrolysis is a not spontaneous process ($\widetilde{\Delta g}_r > 0$) with an increase of the order ($\widetilde{\Delta s}_r < 0$) passing from the reactant (H₂O) to the products (H₂ and O₂). Hence, to realize the process, is needed an energy per molar unit of reactant expressed by the molar enthalpy of reaction:

$$\widetilde{\Delta h}_r = \widetilde{\Delta g}_r - T\widetilde{\Delta s}_r > 0$$

Thus, the chemical process is endothermic, with part of the energetic input ($\widetilde{\Delta g}_r$) stored inside the products as chemical energy and part ($-T\widetilde{\Delta s}_r$) required as the heat of reaction. Since, in an electrolyser, this input is in form of electricity, it is convenient to express the contributions in terms of powers, by means of the Faraday Law:

$$\dot{n}_{H_2O} = \frac{I}{Z_{F,H_2O} F}$$

Where

- $I [A]$ is the electric current circulating in the circuit of the electrolyser;
- $Z_{F,H_2O} = 2$ is the number of charge carries per unit mole of water;
- $F = 96487 \left[\frac{C}{mol} \right]$ is the Faraday constant.

Then

$$\frac{\widetilde{\Delta h}_r}{Z_{F,H_2O} F} I = \left(\frac{\widetilde{\Delta g}_r}{Z_{F,H_2O} F} - T \frac{\widetilde{\Delta s}_r}{Z_{F,H_2O} F} \right) I$$

where the *chemical power stored inside the products* is

$$\dot{Q}_u = \frac{\widetilde{\Delta g}_r}{Z_{F,H_2O} F} I$$

while the *thermal power of reaction* is (passing to the convention of positive heat when enters the process, negative when exits):

$$\dot{Q}_r = T \frac{\widetilde{\Delta s}_r}{Z_{F,H_2O} F} I$$

2. *Transport processes' contribution*: at open circuit, the voltage at the electrodes of the electrolyser is:

$$OCV = \frac{\widetilde{\Delta g}_r}{Z_{F,H_2O} F}$$

However, closing the circuits, some processes (related to catalyst's activation at low currents, ohmic resistance at intermediate ones and diffusion limitations at high ones) hinder the functioning of the electrolyser. These phenomena are expressed in terms of overpotentials β_j , so that the polarization curve of the electrolyser is expressed as:

$$V_c = \frac{\widetilde{\Delta g}_r}{Z_{F,H_2O} F} + \sum_j^3 \beta_j$$

The overpotentials produce a release of thermal power (passing to the convention of positive heat when enters the process, negative when exits):

$$\dot{Q}_{irr} = - \sum_j^3 \beta_j I$$

In conclusion, the *thermal power exchanged by the system* is:

$$\dot{Q}_c = \dot{Q}_r + \dot{Q}_{irr} = \left[\frac{\widetilde{\Delta h}_r}{Z_{F,H_2O} F} - V_c \right] I$$

The point where it is null is called *thermoneutral point*.

References

Arab, S., Commenge, J.-M., Portha, J.-F. & Falk, L., 2014. Methanol synthesis from CO₂ and H₂ in multi-tubular fixed-bed reactor and multi-tubular reactor filled with monoliths. *Chemical Engineering Research and Design*, 92(11), pp. 2598-2608.

Atsonios, K., Panopoulos, K. D. & Kakaras, E., 2016. Investigation of technical and economic aspects for methanol production through CO₂ hydrogenation. *International Journal of Hydrogen Energy*, 4 January, 41(4), pp. 2202-2214.

Audi, n.d. *Audi Tecnology Portal*. [Online]

Available at: https://www.audi-technology-portal.de/en/mobility-for-the-future/audi-future-lab-mobility_en/audi-future-energies_en/audi-e-gas_en

[Accessed 20 November 2018].

Behrens, M. et al., 2012. The Active Site of Methanol Synthesis over Cu/ZnO/Al₂O₃ Industrial Catalysts. *SCIENCE*, 336(6083), pp. 893-897.

Benenati, R. F. & Brosilow, C. B., 1961. Void Fraction Distribution in Beds of Spheres. *A.I.Ch.E. Journal*, 8(3), pp. 359-361.

Bird, R. B., Stewart, W. E. & Lightfoot, E. N., 2002. *Transport phenomena*. II ed. New York / Chichester / Weinheim / Brisbane / Singapore / Toronto: John Wiley & Sons.

British Petroleum Company, 2017. *BP Statistical Review of World Energy 2017*. [Online]

Available at: <http://www.bp.com/en/global/corporate/energy-economics/statistical-review-of-world-energy.html>

[Accessed 19 September 2017].

Calì, M. & Gregorio, P., 1996. *Termodinamica*. s.l.:Società Editrice Esculapio.

CAMEO chemicals, n.d. *DIMETHYL ETHER*. [Online]

Available at: <https://cameochemicals.noaa.gov/chemical/585>

[Accessed 2018 September 2018].

contributors, W., 2018. *Carbon capture and storage*. [Online]

Available at: https://en.wikipedia.org/wiki/Carbon_capture_and_storage

[Accessed 29 August 2018].

contributors, W., 2018. *Fossil fuel*. [Online]

Available at: https://en.wikipedia.org/w/index.php?title=Fossil_fuel&oldid=855936956

[Accessed 23 August 2018].

contributors, W., 2018. *Industrial Revolution*. [Online]

Available at: https://en.wikipedia.org/w/index.php?title=Industrial_Revolution&oldid=854515582

[Accessed 22 August 2018].

- Elkamel, A., Zahedi, G. R., Marton, C. & Lohi, A., 2009. Optimal Fixed Bed Reactor Network Configuration for the Efficient Recycling of CO₂ into Methanol. *Energies*, 2(2), pp. 180-189.
- European Commission, Secretariat-General, 2016. *COMMUNICATION FROM THE COMMISSION TO THE EUROPEAN PARLIAMENT AND THE COUNCIL The Road from Paris: assessing the implications of the Paris Agreement and accompanying the proposal for a Council decision on the signing, on behalf of the European Union, of th.* [Online]
Available at: <https://eur-lex.europa.eu/legal-content/EN/TXT/?uri=CELEX:52016DC0110>
[Accessed 28 August 2018].
- Ferrari, G., 2016. *Motori a combustione interna*. s.l.:Società Editrice Esculapio.
- Finlayson, B. A., 2012. *Introduction to chemical engineering computing*. II ed. s.l.:John Wiley & Sons.
- Froment, G. F., Bischoff, K. B. & De Wilde, J., 2010. *Chemical Reactor Analysis and Design*. III ed. s.l.:Wiley.
- Gaikwad, R., Bansode, A. & Urakawa, A., 2016. High-pressure advantages in stoichiometric hydrogenation of carbon dioxide to methanol. *Journal of Catalysis*, Volume 343, pp. 127-132.
- Giacosa, D., 2000. *Motori endotermici*. s.l.:HOEPLI EDITORE.
- Graaf, G. H., Scholtens, H., Stamhuis, E. J. & Beenackers, A. A. C. M., 1990. Intra-particle diffusion limitations in low-pressure methanol synthesis. *Chemical Engineering Science*, 45(4), pp. 773-783.
- Graaf, G. H. & Winkelman, J. G. M., 2016. Chemical Equilibria in Methanol Synthesis Including the Water-Gas Shift Reaction: A Critical Reassessment. *Industrial & Engineering Chemistry Research*, 55(20), pp. 5854-5864 .
- Green, D. W. & Perry, R. H., 2007. *Perry's Chemical Engineers' Handbook, Eighth Edition*. 8 ed. s.l.:McGraw Hill Professional,.
- He, W., Lu, W. & Dickerson, J., 2014. Gas Diffusion Mechanisms and Models. In: *Gas Transport in Solid Oxide Fuel Cells*. s.l.:Springer, Cham.
- Huaman, R. N. E. & Lourenco, S., 2015. A Review on: CO₂ Capture Technology on Fossil Fuel Power Plant. *Journal of Fundamentals of Renewable Energy and Applications*, 5(164).
- HYDROGENICS, 2017. *Renewable Hydrogen Solutions*. [Online]
Available at: <https://solutions.hydrogenics.com/renewable-hydrogen-solutions-brochure?hsCtaTracking=e0d8363e-ee2c-4a34-a247-9ff4b9913e64%7Cc6913d5e-6eb7-443b-81c2-f14f1b779485>
[Accessed 21 November 2018].
- Jadhava, S. G., Vaidyaa, P. D., Bhanageb, B. M. & Jyeshtharaj B. Joshia, 2014. Catalytic carbon dioxide hydrogenation to methanol: A review of recent studies. *Chemical Engineering Research and Design*, 92(11), pp. 2557-2567.

Joghee, P., Malik, J. N., Pylypenko, S. & O'Hayre, R., 2015. A review on direct methanol fuel cells – In the perspective of energy and sustainability. *MRS Energy & Sustainability*, 2(e3).

Kobl, K. et al., 2016. Power-law kinetics of methanol synthesis from carbon dioxide and hydrogen on copper–zinc oxide catalysts with alumina or zirconia supports. *Catalysis Today*, Volume 270, pp. 31-42.

Leung, D. Y., Caramanna, G. & Maroto-Valer, M. M., 2014. An overview of current status of carbon dioxide capture and storage technologies. *Renewable and Sustainable Energy Reviews*, Volume 39, pp. 426-443.

Lim, H.-W. et al., 2010. Optimization of methanol synthesis reaction on Cu/ZnO/Al₂O₃/ZrO₂ catalyst using genetic algorithm: Maximization of the synergetic effect by the optimal CO₂ fraction. *Korean Journal of Chemical Engineering*, 27(6), p. 1760–1767.

Lim, H.-W. et al., 2009. Modeling of the Kinetics for Methanol Synthesis using Cu/ZnO/Al₂O₃/ZrO₂ Catalyst: Influence of Carbon Dioxide during Hydrogenation. *Industrial & Engineering Chemistry Research*, 48(23), pp. 10448-10455.

Liu, X.-M., Lu, G. Q., Yan, Z.-F. & Beltramini, J., 2003. Recent Advances in Catalysts for Methanol Synthesis via Hydrogenation of CO and CO₂. *Industrial & Engineering Chemistry Research*, 42(25), pp. 6518-6530.

Mcsweeney, R. & Pearce, R., 2016. *Analysis: Only five years left before 1.5C carbon budget is blown*. [Online]

Available at: <https://www.carbonbrief.org/analysis-only-five-years-left-before-one-point-five-c-budget-is-blown>

[Accessed 28 August 2018].

Methanex, 2015. *About Methanol*. [Online]

Available at: <https://www.methanex.com/about-methanol>

[Accessed 5 October 2017].

Methanol Institute, n.d. *Physical Properties of Pure Methanol*. [Online]

Available at: <http://www.methanol.org/methanol-properties/>

[Accessed 4 October 2017].

National Center for Biotechnology Information, n.d. *PubChem Compound Database*. [Online]

Available at: <https://pubchem.ncbi.nlm.nih.gov/compound/8254>

[Accessed 27 September 2018].

Natta, G., Pasquon, I. & Centola, P., 1978. *Principi della chimica industriale*. Milano: clup.

Olah, G. A., Goeppert, A. & Prakash, G. K. S., 2009. Chemical Recycling of Carbon Dioxide to Methanol and Dimethyl Ether: From Greenhouse Gas to Renewable, Environmentally Carbon Neutral Fuels and Synthetic Hydrocarbons. *JOC Perspective*, 16 January, 74(2), p. 487–498.

- Pérez-Forte, M., Schöneberger, J. C., Boulamanti, A. & Tzimas, E., 2016. Methanol synthesis using captured CO₂ as raw material: Techno-economic and environmental assessment. *Applied Energy*, Volume 161, pp. 718-732.
- Poling, B. E., Prausnitz, J. M. & O'Connell, J. P., 2001. *The properties of gases and liquids*. V ed. s.l.:McGraw-Hill.
- Raudaskoski, R. et al., 2009. Catalytic activation of CO₂: Use of secondary CO₂ for the production of synthesis gas and for methanol synthesis over copper-based zirconia-containing catalysts. *Catalysis Today*, 144(3-4), pp. 318-323.
- Ritchie, H., 2017. *How long before we run out of fossil fuels?*. [Online]
Available at: <https://ourworldindata.org/how-long-before-we-run-out-of-fossil-fuels/>
[Accessed 28 August 2018].
- Ritchie, H. & Roser, M., 2017. *Energy Production & Changing Energy Sources*. [Online]
Available at: <https://ourworldindata.org/energy-production-and-changing-energy-sources/>
[Accessed 21 September 2017].
- Saeidi, S., Saidina Amin, N. A. & Rahimpour, M. R., 2014. Hydrogenation of CO₂ to value-added products—A review and potential future development. *Journal of CO₂ Utilization*, 22 gennaio, Volume 5, pp. 66-81.
- Treccani, n.d. *Tensione*. [Online]
Available at: <http://www.treccani.it/enciclopedia/tensione>
[Accessed 07 10 2017].
- Van-Dal, É. S. & Bouallou, C., 2013. Design and simulation of a methanol production plant from CO₂ hydrogenation. *Journal of Cleaner Production*, Volume 57, pp. 38-45.
- Wang, W., Wang, S., Ma, X. & Gong, J., 2011. Recent advances in catalytic hydrogenation of carbon dioxide. *Chem. Soc. Rev.*, 40(7), pp. 3703-3727.
- Yanju, W. et al., 2008. Effects of Methanol/Gasoline Blends on a Spark Ignition Engine Performance and Emissions. *Energy & Fuels*, 22(2), pp. 1254-1259.
- Zhen, X. & Wang, Y., 2015. An overview of methanol as an internal combustion engine fuel. *Renewable and Sustainable Energy Reviews*, Volume 52, pp. 477-493.

Ringraziamenti

Finalmente ho raggiunto il traguardo: la laurea è mia! Questi anni di università sono stati molto impegnativi e, in alcune occasioni, mi hanno messo seriamente alla prova. Tuttavia, anche nei momenti più duri, ho sempre avuto persone che credessero in me, mi sostenessero e, talvolta, affrontassero le mie stesse sfide. Dunque, sento di dover ringraziare molte persone. Da degno studente di ingegneria, ringrazierò in modo molto organizzato: non in ordine di importanza (sarebbe impossibile), ma per compartimenti della mia vita. Innanzitutto, voglio ringraziare Nico e Davide, i miei “fratelli in armi”. Abbiamo condiviso momenti durissimi, progetti che parevano infiniti, sessioni in cui si andava avanti per inerzia. Tuttavia, ci sono stati anche molti episodi divertenti: le ricerche dei posti in aula studio, con il mio “radar” sempre attivo e Davide che attaccava bottone con chiunque, usando le mentine come espediente. Io che prendevo appunti durante le lezioni, mentre Nico passava in modalità PR e organizzava feste. Le giornate in cui ci trovavamo tutti e tre a casa di Davide per studiare, con quel misto di concentrazione e disperazione degli studenti pochi giorni prima di un esame, ma poi, arrivata la pausa pranzo, ecco che cambiava il registro: tra il troppo cibo, la bottiglia di vino, il combattimento con Da, le sfide a freccette, le trazioni alla sbarra e il collasso sul divano, la tensione si allentava molto (per non parlare della concentrazione nella prima oretta di studio del pomeriggio). Tra l’altro, un particolare ringraziamento va a Davide: ho cercato per secoli un abito per la laurea e, quando gli ho telefonato, disperato, chiedendogli di accompagnarmi a cercarne uno, si è reso subito disponibile e, in venti minuti (più un’ora e mezza di ricerca del parcheggio), l’abbiamo trovato. Poi voglio ringraziare Jole, Paolo e Gianluca. Quanti momenti passati assieme... E il bello è che, tra Jole che andava in panico all’ennesima potenza, Paolo che diceva che gli piaceva quando gli spiegavo le cose perché avevo una voce che lo tranquillizzava e Gianluca avvilito dalla mole di cose da fare, io risultavo essere quello ottimista (io?!). E come non ringraziare Sara, Roberta, Federica e Nicola, che non mi hanno ammazzato, nonostante mi abbiano sentito parlare non so quante volte della mia tesi e si siano sentiti dire spesso: “Stasera non posso uscire, mi dispiace: sono pieno di lavoro da fare”. Bisogna recuperare! Passiamo poi a Fe ed Eddy (gli amici di una vita) e Fra, con cui puoi parlare di tutto (dalla politica, a inizio serata, alle “invenzioni innovative”, a fine serata). Molte volte mi hanno tirato su il morale in momenti di forte preoccupazione e hanno smosso mari e monti per poter essere presenti alla mia laurea. Grazie mille, ragazzi! Adesso tocca a Je, che mi conosce da 19 anni e si è goduta tutti i miei scleri con la scuola (la maturità rimarrà negli annali), alcuni dei miei “migliori” momenti (ho capito che è meglio stare lontani da fontane, scogli e cani con te) e che, ogni volta che ci siamo incontrati, è stata in grado di chiedermi con convinzione (sapendo già la risposta): “E la tesi come va?”. Grazie. Passiamo adesso alla famiglia. È ovvio: sono stati i miei parenti a fare di me quel che sono, a darmi la curiosità, la testardaggine, la voglia di fare, l’ambizione, l’etica del lavoro e l’orgoglio che mi hanno consentito di laurearmi; diciamo che anche il fare polemico di alcuni di loro (non li cito per eleganza, ma immagino che qualcuno si riconosca in questa caratteristica) mi ha aiutato ad affrontare con fiducia in me stesso (o sfrontataggine) alcune situazioni difficili. Ovviamente, il ringraziamento più grande va ai miei genitori, che mi hanno consentito di frequentare l’università, sostenendomi sempre, credendo in me più di quanto io facessi, ascoltando i miei fiumi di parole su questa o quella cosa che mi aveva fatto infuriare o mi preoccupava. Riconosco che avere un universitario in casa non deve essere stato facile, ma se la sono cavata molto bene. Una delle cose che mi hanno insegnato è mettere tutto sé stesso nel raggiungimento dei propri obiettivi e

puntare più in alto possibile, senza limitarsi per paura di non farcela. L'ho fatto all'università e lo farò nel lavoro. Ma per adesso, mi limiterò a festeggiare!